REVIEW

**ADVANCED
MATERIALS**

www.advmat.d

Check for
updates

Hydrogel Bioink Reinforcement for Additive Manufacturing: A Focused Review of Emerging Strategies

David Chimene, Roland Kaunas, and Akhilesh K. Gaharwar*

Bioprinting is an emerging approach for fabricating cell-laden 3D scaffolds via robotic deposition of cells and biomaterials into custom shapes and patterns to replicate complex tissue architectures. Bioprinting uses hydrogel solutions called bioinks as both cell carriers and structural components, requiring bioinks to be highly printable while providing a robust and cell-friendly microenvironment. Unfortunately, conventional hydrogel bioinks have not been able to meet these requirements and are mechanically weak due to their heterogeneously crosslinked networks and lack of energy dissipation mechanisms. Advanced bioink designs using various methods of dissipating mechanical energy are aimed at developing next-generation cellularized 3D scaffolds to mimic anatomical size, tissue architecture, and tissue-specific functions. These next-generation bioinks need to have high print fidelity and should provide a biocompatible microenvironment along with improved mechanical properties. To design these advanced bioink formulations, it is important to understand the structure–property–function relationships of hydrogel networks. By specifically leveraging biophysical and biochemical characteristics of hydrogel networks, high performance bioinks can be designed to control and direct cell functions. In this review article, current and emerging approaches in hydrogel design and bioink reinforcement techniques are critically evaluated. This bottom-up perspective provides a materials-centric approach to bioink design for 3D bioprinting.

1. Introduction

3D printing was first made a reality in the 1980's when Charles Hull developed stereolithography, a technique for converting 3D computer-aided design into physical objects by projecting a series of light patterns into a pool of photopolymers.[1] This development was quickly followed by the emergence of other 3D fabrication strategies, including fused deposition modeling (FDM) in 1989, which builds objects by precisely depositing successive layers of molten thermoplastic using a mobile heated nozzle.[2] FDM has evolved to become the most popular 3D printing technique due to its low cost and accessibility, and has experienced a rapid explosion in popularity since its patent expiration in 2009. Since then, open source designs like RepRap printers ("Replicating Rapid-Prototyper"), which can 3D print many of their own components, have dramatically driven down printer costs from the tens of thousands of dollars to fewer than 200 dollars. This has brought the technology into the hands of millions of hobbyists and academics alike. The widespread adoption of 3D printing technology has led to its application to new fields, including regenerative medicine. 3D printers are being commercialized to rapidly create custom prosthetics for patients and to precisely replicate patient anatomy to allow surgeons to simulate procedures with 3D printed body parts. Most recently, 3D printing has been adopted for tissue engineering with the goal of developing highly customized cell-laden scaffolds to enable healthy human tissue to be regrown from a patient's own stem cells. This technique of 3D printing living cells is called 3D bioprinting.

3D bioprinting can localize different cell types and materials to mimic the anatomical complexity of tissues and organs.[3–5] 3D bioprinting living cells requires a very specific set of conditions that are best met by a certain class of materials: hydrogels. For example, cells require an aqueous environment, and sufficient oxygen and nutrient diffusion, as well as appropriate pH and osmolarity along with key vitamins and minerals for cellular functions. Certain cell types require specific cell attachment sites and substrate properties in order to proliferate. Finally, cells must have room to create new extracellular matrix. This means that printed materials should degrade into nontoxic components over time to promote new tissue formation.[6–8]

Hydrogels are able to meet these stringent requirements and are the basis of almost all bioink formulations. Hydrogels are loosely crosslinked networks of highly hydrophilic polymers

D. Chimene, Prof. R. Kaunas, Prof. A. K. Gaharwar
Biomedical Engineering
Dwight Look College of Engineering
Texas A&M University
College Station, TX 77843, USA
E-mail: gaharwar@tamu.edu
Prof. A. K. Gaharwar
Material Science and Engineering
Dwight Look College of Engineering
Texas A&M University
College Station, TX 77843, USA
Prof. A. K. Gaharwar
Center for Remote Health Technologies and Systems
Texas A&M University
College Station, TX 77843, USA

The ORCID identification number(s) for the author(s) of this article can be found under https://doi.org/10.1002/adma.201902026.

that can absorb many times their dry weight in water, generally ranging from 70% to over 99% water content. This high water content makes hydrogels highly porous and permeable, allowing rapid diffusion of oxygen and nutrients throughout the scaffold.[7,8] Many hydrogels are also porous enough to allow cell migration, and some are also degradable, providing initial support for cells, then degrading away as cell populations grow and remodel their surroundings. Hydrogels can also be created from proteins and extracellular matrix components, including collagen and hyaluronic acid (HA), providing environmental cues to help direct stem cell growth. Finally, many hydrogels can be crosslinked into solid viscoelastic structures using cell-friendly methods, which are not damaging to living cells and minimize physiological stress on printed cells encapsulated within the scaffold. These characteristics allow hydrogels to closely mimic the native microenvironment of cells, making them the nearly universal choice for 3D bioprinting.[8–11]

Conventional hydrogels are randomly crosslinked, single network hydrogels with no internal mechanism for mechanical energy dissipation, and make up the majority of hydrogels used in biomedical research. While conventional hydrogels are inherently suited for cell growth, they lack mechanical properties needed for optimal 3D printing. Adapting them to 3D printing has therefore proven to be a consistent challenge to the field. Prior to crosslinking, hydrogels are typically liquid polymer solutions, making it impossible to support subsequent layers. Many conventional hydrogels crosslink too slowly or remain too weak to be practical for structures taller than a few millimeters. Hydrogel networks are conventionally strengthened by increasing their polymer content and crosslink density; however, increased polymer content and dense crosslinks interfere with cell culture by reducing the permeability and porosity that cells require. Crosslinks also form randomly in conventional hydrogels, causing variations in crosslink density that concentrate stress on the least extensible chains under deformation.[7,8,11] These factors make conventional hydrogel reinforcement undesirable in bioinks.

This compromise between biocompatibility and printability properties to make acceptable bioinks is often thought of as a biofabrication window. However, new approaches are being developed to improve the biofabrication window by efficiently strengthening hydrogels while retaining favorable biological properties (**Figure 1**a). The most popular techniques include polymer functionalization, interpenetrating networks (IPNs), nanocomposites, supramolecular bioinks, and thermoplastic reinforcement. While multiple reviews of bioinks currently exist, they lack a mechanistic approach to structure–property–function relationships in bioinks.[7,8,11]

The bioink reinforcement techniques discussed in this review exhibit enhanced performance brought about by distinct network structures, but they also share some fundamental traits. A general principle for tough hydrogels is that they can relax stress concentrations and dissipate mechanical energy, increasing the energy required before cracks form and propagate. This is important for bioink reinforcement because it means fracture energy depends not just on the energy needed to break the polymer chains in a propagating crack's path, but also on the amount of mechanical energy that the surrounding region can dissipate. Bioink literature does not always report
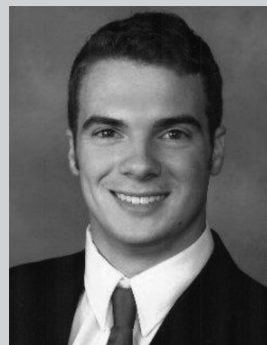
David Chimene is a doctoral candidate at Texas A&M University in the Department of Biomedical Engineering. His research focuses on bioink design, biomaterials, hydrogels, nanomaterials, and 3D bioprinting. He is currently designing efficient bioink reinforcement, and engineering low-cost bio-printers to expand bioprinting's accessibility.

Roland Kaunas is an Associate Professor and Director of Graduate Programs in the Department of Biomedical Engineering at Texas A&M University. His laboratory focuses on the engineering of microtissues containing mesenchymal stem cells for regenerating musculoskeletal tissues and as cell-based models for studying tumor biology. This work employs sophisticated microfluidic platforms, custom bioreactors, and novel scaffolding strategies involving composites of natural and synthetic polymers.

Akhilesh K. Gaharwar is an Associate Professor in the Department of Biomedical Engineering at Texas A&M University. He received his Ph.D. from Purdue University and completed his postdoctoral training from Massachusetts Institute of Technology and Harvard University. The goal of his lab is to design next generation of biomaterials to harnesses the body's innate regenerative potential for repair or replacement of damaged tissues by combining principles from materials science, additive biomanufacturing, stem cell biology, and high throughput genomics. Specifically, he has contributed to fundamental design and application of 2D nanomaterials—important for the development of bioresponsive and shear-thinning biomaterials.

fracture energy, so we discuss available mechanical measures when necessary.

Bioinks assume multiple functions key to bioprinting success, many of which are interrelated through properties

affecting the hydrogel structure. However, existing literature has not adequately explored these relationships. In this review, we bridge this literary gap by examining the relationships between a bioink's hydrogel structure, properties, and function. We critically examine how the fundamental concepts of hydrogel network structures relate to the mechanical, rheological, and biological properties that are critical to bioprinting success. Then we discuss specific emerging bioink reinforcement mechanisms and their effects on key bioink properties. Finally, we evaluate promising approaches to next-generation bioink designs. Understanding the fundamental mechanisms of hydrogel reinforcement and how they can be applied to design advanced bioinks will provide an in-depth understanding of trends emerging in the development of high performance bioinks.

2. Bioink Characteristics

The cell-friendly nature of hydrogels has made them the material of choice for printing 3D cell constructs.[9,12,13] Hydrogels consist of highly hydrophilic polymer networks that can absorb many times their own weight in water. They are used in a wide range of commercial products, ranging from baking and food additives to medical devices. Hydrogel networks can be held together in their solid state by physical and/or covalent interactions called crosslinks. The mechanical properties of these crosslinked networks are determined by complex interactions between the polymer network structure and aqueous components. Before hydrogels form crosslinks, they exist as polymer solutions that can have fluid-like properties (also known as sols) that depend on their composition. This is typically the state of a bioink during extrusion (Figure 1b). Controlling both the noncrosslinked solution (bioink) fluid properties and the crosslinked hydrogel (structure or, when bioprinted, scaffold) mechanical properties is a major focus of bioprinting research.

In this section we will review key rheological, structural, biomechanical, and biochemical properties of bioinks, and discuss how they are related to bioink performance. It is important to recognize that these properties are interrelated in complex ways that must be considered when optimizing bioink performance. As research on bioinks has progressed, certain factors in each of these areas have been widely identified as critical to bioink performance (e.g., shear thinning and elastic modulus); others are still being evaluated (e.g., shear recovery and stress relaxation). While many of these factors are not consistently reported in bioprinting literature, they are nevertheless beneficial to consider when evaluating bioink designs.

2.1. Hydrogel Bioink Network and Design Parameters

We begin by describing the fundamental mechanics of hydrogel networks to better contextualize discussions of reinforcement strategies in later sections.[14–18] Polymer networks have been widely used in engineering since the 1840s, when Charles Goodyear developed the first elastomers through rubber vulcanization. The vulcanization process crosslinks the network to prevent polymer chains from flowing, effectively solidifying the

rubber across a wide range of temperatures. Elastomers remain the most widely used polymer networks today, with applications ranging from tires to disposable surgical gloves.[14] In contrast, the history of hydrogel polymer networks is much shorter and intimately tied to biomedical engineering. Synthetic hydrogels were first engineered in the 1950's when hydroxyethyl methacrylate was developed as a contact lens material, and their potential for mimicking the body's natural environment was quickly investigated.[19] The range of biomedical applications involving hydrogels quickly expanded to include burn treatments, drug delivery, cosmetics, and implants.[20,21] Hydrogel research has grown exponentially over the past few years due to their application to regenerative medicine and bioprinting.[20] Like elastomers, hydrogels are essentially polymer chains whose flow is prevented by crosslinks that provide elastic strength.[14]

2.1.1. Soft Network Basics

Classical polymer networks are mainly formed in two ways: by simultaneous polymerization and crosslinking of a monomer solution, and by crosslinking existing polymer chains together. Both methods generally create randomly crosslinked, heterogeneous networks containing both densely and sparsely crosslinked regions.[14] Upon loading, this heterogeneity leads to localized stress concentrations that form weaker failure zones in the polymer network. Thus, the distribution of crosslinks is a key determinant to polymer network mechanical properties. Individual polymer chains behave like entropic springs whose elasticity is dependent on their configurational degrees of freedom. While crosslinking increases the number of polymer chains in a network, the individual chains become shorter, thus lowering configurational entropy and creating a stiffer and more brittle network.[14] The energy required to break a polymer chain is proportional to its length. Shorter polymer chains also constrain the extensibility of the network. The overall impacts of these competing effects of crosslinking are increases in tensile strength at the price of reduced threshold fracture energy. In other words, extensive crosslinking makes conventional hydrogels stiff and brittle while loosely crosslinked hydrogels are softer but relatively tough.[15,17] Thus, while crosslinks are vital to polymer network structure, increased crosslinking leads to a random, heterogeneous network structure and rapidly decreases extensibility, causing brittleness and adversely affecting mechanical reinforcement.[14,18]

2.1.2. Fracture Energy and Energy Dissipation

Current bioink literature often characterizes gels with just a few mechanical parameters, such as fracture strain and stress, and compressive, tensile, or shear moduli. These parameters are important, but only partially describe the mechanical properties of a hydrogel. A parameter that is particularly useful for comparing overall mechanical properties in polymer networks is fracture energy, alternatively referred to as tearing energy or critical strain energy release rate.[18] Fracture energy describes the amount of energy required to perpetuate a fracture through
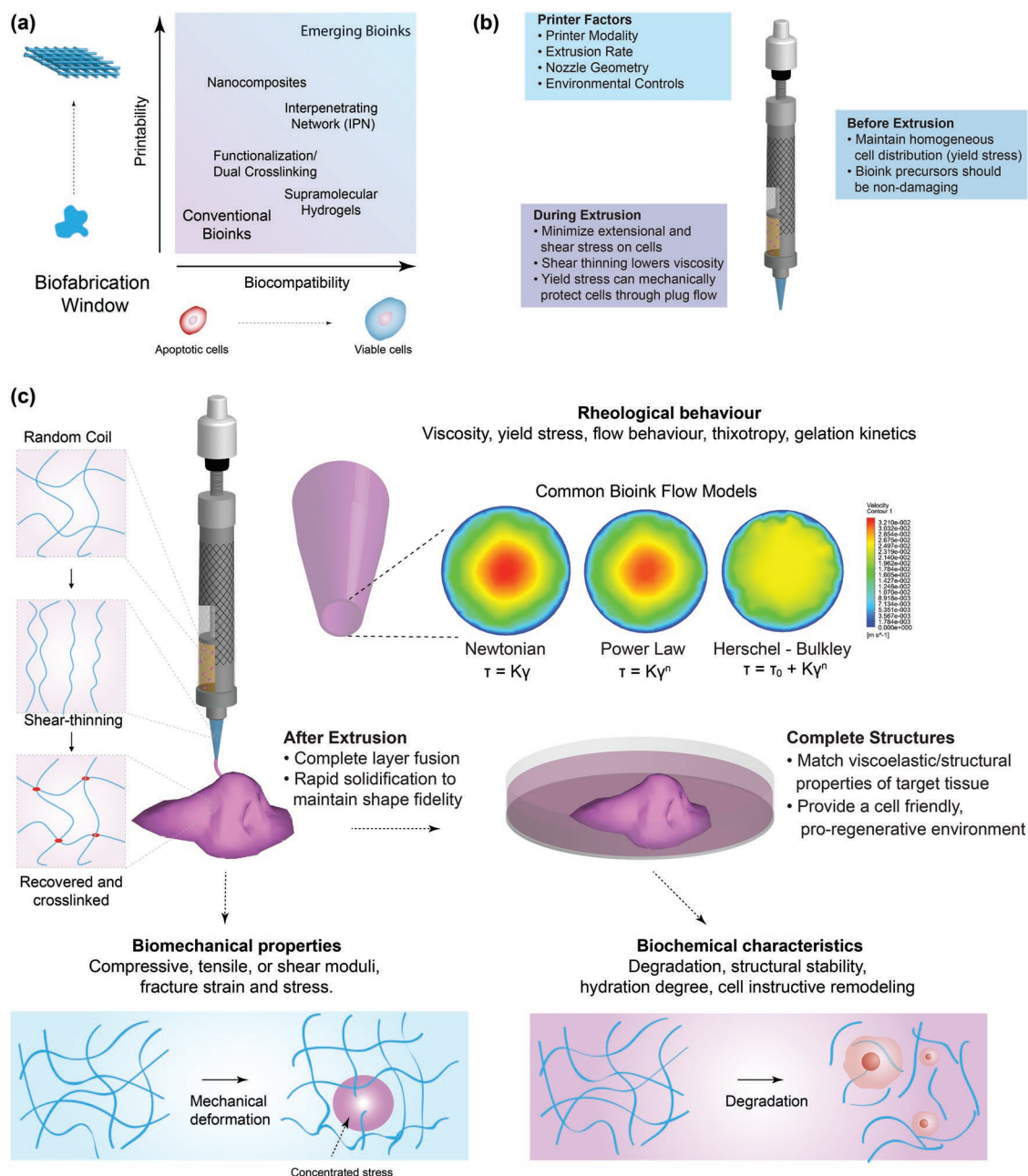
Figure 1. Hydrogel bioink design consideration reinforcement approaches. a) The biofabrication window depicts the compromise between printability and biocompatibility needed to make acceptable bioinks. Emerging bioink reinforcement techniques improve fabrication while maintaining biocompatibility. b) Bioink considerations at different fabrication stages. A range of printing factors can determine success or failure of a bioprint. c) The rheological, biomechanical, and biochemical characteristics of bioinks play major roles in extrusion bioprinting. The structural and mechanical properties of a bioink are key metrics of its performance at both the macro- and microscale, influencing everything from structural integrity to biomechanical and biochemical cellular interactions. Mechanical reinforcement also significantly affects a bioink's 3D printability by altering its flow properties. The most common bioink flow models include Newtonian, Power Law, and Herschel–Bulkley fluids. Bioink flow properties significantly alter flow velocity profiles during printing and determine the amount of stress that encapsulated cells experience during the printing process, and also impact 3D printability through viscoelastic behavior after extrusion.

the network. It is defined as the energy required to create a unit area of crack growth (J m^{-2}).[15,16] Fracture energy is an attractive metric because it is an intrinsic material property that is independent of geometry and is thus generally consistent across different test methods.

In polymer networks, fracture energy ($\Gamma(v)$) can be divided into two components according to its governing equation (Equation (1))[14]

$$\Gamma(v) = \Gamma_0 \left(1 + \varphi(a_\mathrm{T} v)\right), \text{ alternatively written as } \Gamma = \Gamma_0 + \Gamma_\mathrm{D} \qquad (1)$$

**ADVANCED
SCIENCE NEWS**

www.advancedsciencenews.com

**ADVANCED
MATERIALS**

www.advmat.de

In Equation (1), $\Gamma_0 = N_x\, U_b\, \Sigma$ and $\Gamma_D = \Gamma_0\, \varphi(a_T \nu)$

The first component, the threshold (or intrinsic) fracture energy (Γ_0), is defined as the amount of energy required to break the polymer chains per unit area of the crack plane as it propagates. The required energy depends on the density of polymer chains crossing the crack plane (Σ), the number of bonds in those polymer chains (N_x), and the energy to break each bond (U_b).[14,15] This energy is local to the area of crack plane path and does not depend on surrounding bulk material. The density of polymer chains in hydrogels is proportional to their volume fraction, giving them a much lower intrinsic fracture energy (≈ 10 J m^{-2}) relative to dry networks (≈ 50–100 J m^{-2}).[15,18]

The second component can be thought of as viscoelastic mechanical energy (Γ_D) dissipated into the surrounding network. Γ_D scales linearly with Γ_0, where $\varphi(a_T \nu)$ is a mechanical dissipation factor that is velocity-and-temperature-dependent and is characteristic of the material.[22] The scaling factor $\varphi(a_T \nu)$ shows a Power Law dependence on crack velocity, so rapid crack propagation requires significantly more energy than gradual crack expansion.[14] Furthermore, Γ_D depends on the bulk properties of the material in the region surrounding the crack. In tough polymer networks, Γ_D can contribute dramatically more to the total fracture energy than Γ_0.[23] For elastomers, the most important mechanism for mechanical energy dissipation is through molecular friction between polymer chains as they translate and rearrange in response to applied stress. Conventional hydrogel networks lack this internal friction mechanism due to the large amount of water between polymer chains, thus leading to rapid crack propagation.[14,15]

In summary, hydrogels share many structural similarities with other soft polymer networks, but their hydrated structure causes their mechanical properties to differ in key ways. In all soft polymer networks, intrinsic fracture energy (Γ_0) depends on the length, number, and bond strength of polymer chains in the crack plane. Crosslinking increases elastic modulus and tensile strength, but reduces fracture energy and extensibility. The low chain density in hydrogels reduces the intrinsic fracture energy (Γ_0) in proportion to polymer volume fraction, and functionally eliminates mechanical energy dissipation (Γ_D) through molecular friction. Together, these severely constrain the mechanical properties of conventional hydrogels.[14]

Fortunately, understanding these structural limitations also provides us with a clear pathway for improving the mechanical properties of hydrogel bioinks by designing novel mechanical energy dissipation mechanisms into the bioink network structure. Incorporating new mechanisms for dissipation can dramatically improve hydrogel stiffness, failure stress, and fracture energy by as many as three orders of magnitude while maintaining a highly extensible network.[16] It is important to recognize that much of the emerging bioink reinforcement technology maintains this common theme: incorporating mechanical energy dissipation (Γ_D) into the hydrogel structure, while maintaining high printability and a cell-friendly environment. Interpenetrating networks, nanocomposites, supramolecular bioinks, and some composite bioinks all share this theme. Intrinsic fracture energy (Γ_0) is also improved by increasing crosslink stability (functionalization) and/or improving network homogeneity (click reactions and sliding crosslinks).[14,15]

2.2. Rheological Characteristics of Bioinks and Flow Modeling

While the effects of mechanical reinforcement on flow properties are often underappreciated, bioink reinforcement cannot be completely understood without also considering these effects.[24–26] During extrusion, bioinks are typically non-crosslinked polymer solutions or even prepolymer solutions. In this section, we discuss the flow characteristics of bioink solutions that determine printability, including viscosity. The viscosity of a bioink is a key characteristic in determining its flow behavior and is among the most commonly measured values during the bioink optimization process. Viscosity can have mixed effects on bioink performance. High viscosity allows extruded bioink to better hold its shape and improves mechanical stability, which is especially beneficial in printing taller structures. However, higher viscosity increases shear stress during printing, which can damage cells by directly disrupting cell membranes and can reduce proliferation in surviving cells. Specifically, shear stresses have been shown to induce morphological changes, cytoskeleton reorganization, and generation of reactive oxygen species, and alter gene and protein expression. This effect is dependent on cell type and density, as well as the level and duration of shear stresses to which cells are exposed.[27] Further, the relatively high resistance to flow can cause the extruder to clog, which contributes to inconsistent ink deposition. Conversely, low viscosity can reduce bioink printability and cause inhomogeneous cell distribution and rapid cell sedimentation.[28,29] Changes in bioink concentration, polymer molecular weight, ion content, temperature, and encapsulated cell density will directly influence bioink viscosity. Thus, all reinforcement techniques are likely to impact viscosity. In addition, we will also discuss other rheological characteristics of bioinks including shear thinning, thixotropy, thermal gelation, and yield stress. We also outline the impact that bioink reinforcement can have on these properties, as well as discuss flow models that help characterize these effects (Figure 1c).

2.2.1. The Newtonian Model

Bioinks that maintain a consistent viscosity over the range of expected print conditions are often modeled using a Newtonian fluid model, where shear rate (γ) is equal to shear stress (τ) divided by viscosity (K). However, this behavior is mostly seen in bioinks with low polymer concentrations, where viscosity is dominated by small, isotropic molecules, or at very low shear rates where Brownian motion can prevent polymer alignment.[8,30] In practice, most bioinks used in extrusion 3D printing are non-Newtonian, meaning that their apparent viscosity depends on shear rate or deformation history. Non-Newtonian effects are generally caused by reorientation of large polymer chains and disruption of electrostatic interactions, which are common features of reinforced bioinks.[29]

2.2.2. The Power Law Model

In shear-thinning bioinks, increasing shear rates force polymer chains to align along the flow direction, which reduces apparent

ADVANCED
SCIENCE NEWS
www.advancedsciencenews.com

ADVANCED
MATERIALS
www.advmat.de

viscosity. The disruption of electrostatic interactions at higher shear rates also decreases apparent viscosity. Shear-thinning properties are beneficial in bioprinting because they combine the high print fidelity of viscous bioinks with high cell viability due to low shear stresses experienced during the bioprinting process. Shear-thinning is more apparent in high molecular weight polymers and at higher polymer concentrations.[8] The simplest method for modeling shear thinning behavior is with the Power Law relationship (Figure 1c), where shear stress (τ) is related to shear rate (γ) by the flow behavior index (n) and consistency index (K), which is the viscosity at 1 s^{-1} shear rate. In this model, $n = 1$ for Newtonian fluids, while n values <1 would be progressively more shear thinning. The Power Law model is useful and simple to use for many bioinks under printing conditions.[26]

2.2.3. The Herschel Bulkley Model

In addition, many non-Newtonian bioinks demonstrate viscoelastic properties like yield stress, which can significantly affect flow behavior. Yield stress is the minimum stress needed to initiate flow. Until shear stress exceeds the yield stress, the bioink behaves like a solid.[8,31] Print fidelity and mechanical integrity are improved by yield stress because the bioink remains solid-like indefinitely after extrusion, even without crosslinking. Additionally, it can shield encapsulated cells from shear forces during extrusion by creating plug flow in the center of the flow profile, thus shearing is confined to a narrow region along the extruder walls.[13,26,31] Very high yield stress can make bioinks difficult to work with. For example, high yield stress interferes with standard pipetting and cell dispersion techniques, requiring alternatives like syringes and manual mixing to be used instead.[13,24] Yield stress behavior in hydrogels is caused by noncovalent and electrostatic interactions, which are frequently a feature of bioink reinforcement. Changes in yield stress have been noted in a range of bioinks, and have been credited with improving bioink printability and cell survival.[13,24] To account for yield stress, a Herschel–Bulkley model is often employed (Figure 1c), which is similar to a Power Law model with an additional term (τ_0) for the yield stress, below which the bioink is assumed to behave as a solid. The Herschel–Bulkley fluid model can accurately map the behavior of non-Newtonian fluids exhibiting shear thinning and yield stress, and has been adopted for bioink modeling in several recent reports.[13,25,28]

2.2.4. Carreau Equation

More complex models can be used for characterizing bioink behavior as well, including the Carreau equation, which is particularly useful for describing different flow behaviors of bioinks at very low and high shear rates. Fluids are treated as Newtonian fluids with constant viscosity when shear rates are too low to overcome the random motion orientation of polymer chains, and as Power Law fluids at intermediate shear rates. At higher shear rates, the fluids become Newtonian again as they reach their infinite shear rate viscosity. This model was recently used to characterize the flow behavior of a polylactide (PLA) microfiber-reinforced alginate bioink.[30,32]

2.2.5. Limitations of Existing Flow Models

While existing flow models can help predict bioink behavior during printing, shear recovery becomes important after extrusion, but is not accounted for in these models.[26] When shear thinning bioinks are deposited after extrusion, their viscosity does not recover instantaneously.[33] Recent papers have demonstrated that rapid shear recovery improves print fidelity by quickly locking extruded bioink in place.[13,26,34,35] Thermoresponsive materials can assist shear recovery by solidifying bioinks in response to a temperature change, which can be exploited to quickly recover viscosity and storage modulus well above their initial values.[13,24]

This effect is particularly evident when bioprinting taller structures where lower layers soon bear the weight of overlying filaments.[13,35–37] This property can be characterized by designing peak-hold experiments to mimic the shear-deformation and recovery of bioink during the printing process.[13,38]

Overall, current flow models are very useful for screening potential bioinks in conjunction with practical experiments. While optimal flow properties vary with experimental goals and print conditions, emerging research indicates that shear thinning, yield stress, and rapid shear recovery are key determinants of bioink printability.[13,24,26,35] These properties are important for successfully bioprinting large-scale, freestanding scaffolds with challenging geometries, including structures with high aspect ratios and overhangs.[13,35–37] Mechanical reinforcement is key to creating next-generation bioinks, but there is still little data on its effects on print performance interactions. Future bioink reinforcement papers can help address this knowledge gap by publishing these rheological properties along with their other experimental results. Current bioink flow models are sufficiently accurate for describing bioink behavior under expected conditions, but do not account for more complex non-Newtonian behaviors like time-dependent effects, thermosensitivity, and wall-slip effects.[26,28,31,39] As bioinks become increasingly complex, more elaborate models should be adopted to more faithfully describe bioink behavior. Rheology and flow modeling are powerful tools to provide scientists a better understanding of the behavior of newly developed bioinks.

2.3. Biomechanical Properties of Bioinks

Due to their high water content, hydrogels used in tissue engineering are softer than many biomaterials, ranging from an elastic modulus <1 kPa for soft collagen gels to >1 mPa for reinforced double network (DN) hydrogels. A desired stiffness is typically achieved by tailoring polymer selection and increasing polymer mass fraction, crosslink density, and molecular weight.[40,41] However, increasing these features generally interferes with the microarchitecture and cytocompatibility of the hydrogels. For example, densely crosslinked hydrogels form stiff structures, but cells become trapped in the network, preventing them from thriving by limiting nutrient diffusion

and restricting space for migration and proliferation. Dense crosslinks also limit flexibility and extensibility of the printed scaffold.[7,8]

2.3.1. Macroscopic Requirements

The mechanical properties of a bioink are crucial to its performance on both the macro- and microscale (Figure 1c). Macroscopically, the eventual goal of bioprinted tissue constructs is implantation into the body, which requires a minimum level of mechanical properties difficult for many bioinks to attain. The ideal mechanical properties of an implant should match those of the target tissue, including stiffness, viscoelasticity, and yield stress/strain. For example, soft tissue implants need to sustain similar levels of compression to the surrounding tissue without failing or separating from surrounding tissue. Especially in bioprinting, hydrogels must also be able to mechanically support themselves after extrusion without significant sagging or deformation, which can interfere with layer-on-layer deposition. A bioink's ability to self-support depends on both its mechanical and rheological properties, as well as crosslinking kinetics.

2.3.2. Cell-Scale Biomechanics

Beyond these macroscopic considerations, the mechanical properties of hydrogels also play an important role in the success or failure of tissue regeneration. For example, elastic modulus (or stiffness) profoundly influences the behavior of encapsulated cells, such as the matrix stiffness-dependent differentiation of mesenchymal stem cells (MSCs).[42,43] Matrix stiffness also plays a key role in tissue repair processes by helping guide fibroblasts and MSCs toward injured tissue and modulating cell proliferation rates.[41] While matrix stiffness has been the primary focus among studies evaluating the effects of mechanical properties on cell-laden scaffolds, emerging research suggests that more complex viscoelastic properties also significantly direct cell behavior. The viscoelasticity of native extracellular matrix plays an important role in regulating cell behavior, and viscoelasticity in hydrogel scaffolds is being likewise recognized for its influence on cell spreading, proliferation, and differentiation. For example, viscoelastic hydrogels demonstrating stress relaxation have been shown to encourage myoblast proliferation even on softer hydrogels when compared to purely elastic hydrogels.[44] Similarly, rapid stress relaxation increases proliferation, spreading, and osteogenic differentiation of MSCs.[45,46]

2.3.3. Extrinsic Mechanical Cues

Extrinsic mechanical signals can also act as biomechanical cues in hydrogels through a process called mechanotransduction.[47,48] Dynamic cyclic 10% compression of MSCs has been shown to promote chondrogenesis, and dynamic deformation has also been shown to induce cell alignment.[49] To complicate matters, cell-material interactions and the intrinsic mechanical properties discussed above can modulate the way cells experience external cues. Timing and duration of mechanical signals can also determine differentiation.[47] The direction and extent of MSC alignment in response to static and cyclic strain is highly dependent on matrix stiffness.[50] Mechanobiology is a quickly growing body of research, but not all research in the area can be applied to bioprinting: 3D cell encapsulation provides a much more complex environment than 2D seeding, and can evoke radically different responses.[46,51] Currently, research on cells encapsulated in hydrogel bioinks focuses primarily on matrix stiffness and viscoelasticity, although this may change as more is learned on this topic.[21,46–49,51]

The structural and biomechanical properties of hydrogel scaffolds are closely related, and structural properties likewise play an important role in determining cell behavior. Pore size and interconnectivity, isotropy, and degradability are all important determinants of cell behavior.[41] Small pore sizes prevent cell migration and reduce nutrient diffusion, while larger pores generally encourage cell migration and proliferation but decrease mechanical properties. Anisotropic features like aligned fibers or pores can also direct cell migration within scaffolds.[52] Finally, biodegradability is also an important consideration, since cells require more space to grow as they progressively generate new tissue, as we discuss below.[21]

2.4. Physiological Stability and Biochemical Interactions of Bioinks

The biochemical environment of a hydrogel is related to biomechanical properties: the biomechanical environment provides cues for cell behavior, and biochemistry can affect the way encapsulated cells respond to these cues (Figure 1c). For example, cells can sense matrix stiffness through integrin proteins, so hydrogels without integrin binding sites diminish cell responses to matrix stiffness.[43,53] Additionally, hydrogel biodegradation is an important factor in hydrogel design. Degradability is desirable in many applications where the hydrogel is meant to be replaced with functional tissue over time. In these instances, the degradation rate should be coupled to the rate of tissue generation to optimize tissue regrowth. Some materials, like peptides, can be enzymatically degraded by cell enzymes that break down extracellular matrix. Other materials, including some polysaccharide networks, degrade through ion exchange that disrupts ionic crosslinks in the hydrogel. Even typically nondegradable polymers, like poly(ethylene glycol) (PEG), can be made to degrade through introduction of hydrolytically sensitive moieties.[54] Overall, the mechanical, structural, and biochemical characteristics of a hydrogel bioink are an important consideration in tissue engineering, and it is important to note that the reinforcement techniques we discuss in this review affect mechanical properties beyond elastic modulus, and research in this area is rapidly developing.[41,45,47,53,55]

3. Bioink Reinforcement Techniques for Additive Manufacturing

The complex and sometimes opposing needs of bioinks have led to a concerted push to invent new ways of incorporating the best possible qualities into bioinks. Early 3D printed

**ADVANCED
SCIENCE NEWS**
www.advancedsciencenews.com
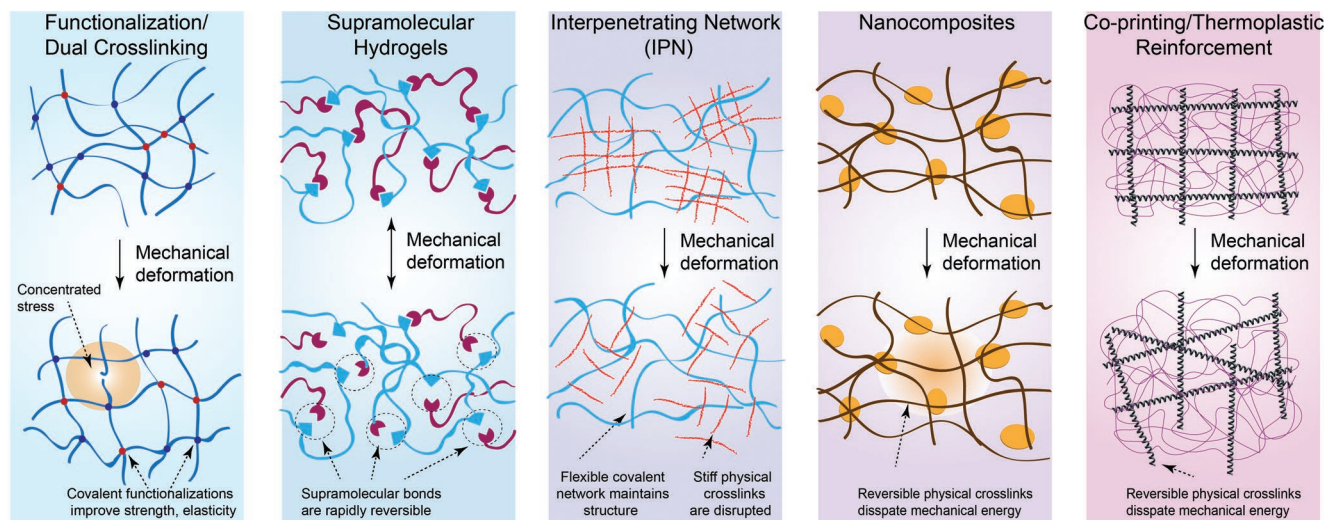
**ADVANCED
MATERIALS**
www.advmat.de

Figure 2. Overview of mechanical reinforcement techniques. Conventional bioinks are typically randomly crosslinked single networks. Established techniques for mechanically reinforcing bioinks include polymer functionalization, supramolecular networks, ionic–covalent entanglement (ICE), nano-composite-based bioink, and co-printing/thermoplastic reinforcement.

hydrogels simply compromised between mechanical properties and cytocompatibility to produce bioinks that were mediocre in both regards. As bioprinting has expanded, there has been a considerable upsurge in development of new techniques to reinforce bioinks through novel technologies. This section will cover emerging trends in bioink reinforcement and how these changes to hydrogel networks affect the key characteristics discussed in the previous section. Specifically, we will discuss bioink reinforcement approaches such as polymer functionalization, supramolecularly reinforced hydrogels, IPNs, nanocomposites, and thermoplastic reinforcement (**Figure 2**). In randomly crosslinked single networks, stress is concentrated in areas with the shortest distances between crosslinks, while slack remains in zones with longer distances between crosslinks. Polymer functionalization can introduce new, stronger crosslinking mechanisms. Sometimes multiple crosslinking mechanisms can be combined to make a dual-crosslinked network. Supramolecular hydrogels incorporate rapidly reversible crosslinks that act as weak points, preventing permanent damage to the network. When ionic–covalent entanglement (ICE) networks are stretched, the physical interactions of the stiffer ionic network are reversibly disrupted to dissipate mechanical energy, resulting in a tougher network. Meanwhile the covalent network maintains hydrogel elasticity. Embedded nanoparticles can act as reversible electrostatic crosslinkers, diffusing stress and dissipating mechanical energy when nanoparticle–polymer bonds are disrupted. Co-printing typically shields and supports weak bioinks, but emerging methods incorporate thermoplastics efficiently at the microscale.

These emerging bioink reinforcement methods improve hydrogel mechanical properties from multiple different approaches, including strengthening crosslinks, homogenizing stress distribution, and dissipating mechanical energy through sacrificial bonds. For example, sliding crosslinks can move in response to applied stress, preventing stress from concentrating

in any one area, thus avoiding premature fracturing of the network. Newer research is also combining multiple bioink reinforcement strategies, for example, by employing both ICE and nanocomposite reinforcement to synergistically improve mechanical properties and printability. Other strategy combinations under development include supramolecular IPNs and nanoreinforced dual-crosslinked bioinks. In the following section, we will briefly discuss the theory behind each reinforcement approach and the recent breakthroughs for their use in bioprinting, as well as outline existing limitations and directions for future development.[14,15]

3.1. Polymer Functionalization and Dual-Crosslinked Networks

One of the most important design shifts during the bioprinting revolution has been the increased use of polymers modified with new chemical moieties. This polymer functionalization can introduce new crosslinking methods and incorporate new biological activity into bioinks. Hydrogels fabricated from synthetic polymers are usually covalently crosslinked networks, while hydrogels from natural polymers are physically crosslinked through conformation changes and physical interactions. Physical crosslinks are weaker than covalent crosslinks but are reversible, and are typically sensitive to environmental factors like temperature, pH, and ion concentrations. Functionalizing natural polymers with covalent crosslinks can improve mechanical properties and reduce sensitivity to environmental conditions. While dual crosslinked networks are single networks that are crosslinked in more than one way, e.g., covalently and ionically in the same network. The permanence and increased bond energy of covalent crosslinks over physical interactions has driven research into incorporating covalent functionalization into natural hydrogels to increase their strength and durability

**ADVANCED
SCIENCE NEWS**

www.advancedsciencenews.com

**ADVANCED
MATERIALS**

www.advmat.de

after 3D printing.[56] Many natural bioinks including alginate, gelatin, hyaluronic acid, and collagen have been reinforced through functionalization to improve mechanical strength and stability in in vivo conditions.[7,57] Polymer functionalization can also be used to modulate properties of bioinks by including sites for degradation and cell attachment. In this section, we will discuss current and emerging approaches to bioink functionalization.

3.1.1. Methacrylate Functionalization

One of the most popular polymer functionalization methods is to incorporate covalent crosslinking by modifying the polymer backbone using methacrylate groups.[58] In this method, a polymer is exposed to methacrylic anhydride to form methacrylate functional groups that can be photocrosslinked in the presence of a photoinitiator. This technique is an attractive modification for adding covalent crosslinking to natural polymers such as gelatin, which is otherwise physically crosslinked through noncovalent bonds below body temperature. Functionalized gelatin methacryloyl (GelMA) maintains many essential bioactive properties of gelatin, including cell attachment and enzymatic degradation.[59] GelMA prints poorly at physiological temperature. However, by leveraging the sol–gel transition of GelMA, cell-laden bioink can be printed into multilayer structures by cooling the bioink to 4 °C for several minutes before printing.[60] In contrast to gelatin, photocrosslinked GelMA is stable at body temperature, has higher fracture energy, is more resistant to degradation, and is able to be photopatterned through selective light exposure.[60,61] The mechanical properties of 3D printed structures using GelMA bioinks can be readily modified by changing polymer concentration, which can be used to direct cell function.[62] 3D vascularized structures can be obtained using sacrificial materials within GelMA hydrogels or microbead-laden hollow GelMA hydrogel fibers.[62]

Methacrylation has been applied to polysaccharides as well, including alginate, HA, and kappa carrageenan (κCA). As most of the acrylated and methacrylated polymers have low viscosity, cure-on-site techniques using UV light have been developed to print these types of polymer bioinks by crosslinking and extruding the bioinks simultaneously. A range of cell-laden, low viscosity bioinks can be bioprinted this way, including methacrylated hyaluronic acid, GelMA, PEG diacrylate (PEGDA), and norbornene-functionalized hyaluronic acid. Interestingly, no significant difference in cell viability was observed between UV photoinitiator and visible light photoinitiator.[63] Polysaccharide hydrogels are generally stiff, but brittle, showing significant plastic deformation and poor recovery upon compressive loading. Covalent functionalization can also decrease stiffness but improve elastic recovery in these bioinks, as demonstrated using a methacrylated κCA bioink.[61,64,65] Covalent functionalization often interferes with the formation of physical crosslinks, which rely on conformation changes that are sensitive to alterations in polymer structure. However, some polymers retain the ability to physically crosslink after functionalization, allowing both crosslinking methods to be combined into a dual-crosslinked network.[60,65,66]

3.1.2. Click Chemistry and other Functionalization Methods

Some bioink functionalization methods utilize click reactions, rather than free radical chain polymerization, to covalently crosslink gelatin polymers.[67,68] Click reactions are a set of synthesis reactions that are highly selective, thermodynamically favorable, and proceed under mild conditions. Thiol-ene click reactions in particular have gained interest for functionalizing biomaterials due to their ease of use and the availability of cysteine residues in peptide polymers.[69] Thiol-ene click reactions are based on reactions between thiols and alkene groups, which can be designed to favor chain transfer over propagation, resulting in a step growth polymerization that recycles radical species.[69] These reactions are not inhibited by oxygen and proceed efficiently at much lower radical concentrations compared to free radical polymerization, which translates to roughly 30x faster crosslinking times in a more cell compatible environment. This rapid crosslinking can improve printability by solidifying extruded bioink within a few seconds of extrusion, reducing structural sagging. The rapid crosslinking kinetics of thiol-ene click reaction has been used to bioprint structures up to 20 layers tall using allylated gelatin.[67] Click crosslinking utilizes a step growth process that creates hydrogels with similar elastic moduli to methacryloyl hydrogels, but produces more homogenous networks, which reduces stress concentrations and has been shown to improve extensibility and fracture toughness.[56,67–70] Finally, there are also non-photocrosslinking agents useful for bioinks. For example, tyrosinase has been used as an alternative to photoinitiator for catalyzing the crosslinking of collagen and gelatins for bioink reinforcement.[71]

To summarize, functionalization reinforces bioinks by introducing covalent crosslinking mechanisms, which are stronger and more stable than physical crosslinks. These reactions are increasingly popular due to the rapid and permanent nature of the crosslinks. Functionalization techniques can improve the fracture energy (Γ) of hydrogel networks, and some reactions, like thiol-ene click reactions, also improve network homogeneity, which increases extensibility. Polymer functionalization improves the network's intrinsic fracture energy (Γ_0) by increasing crosslink bond energy. However, total fracture energy remains relatively low unless it is combined with an energy dissipative mechanism to increase Γ_D, like interpenetrating networks, nanocomposites, or supramolecular bonds. This makes functionalization a common step in fabricating high performance bioinks.

3.2. Supramolecular Bioinks

Sacrificial bonds improve bioink mechanical properties by dissipating stress to increase fracture energy. When these sacrificial bonds show reversible characteristics, the network can potentially resist many cycles of deformation. This is a driving force for development of another interesting class of self-healing inks known as supramolecular bioinks (**Figure 3**). Supramolecular hydrogels are composed of short polymer strands that self-assemble into a network through noncovalent interactions between functional end groups. When these interactions are
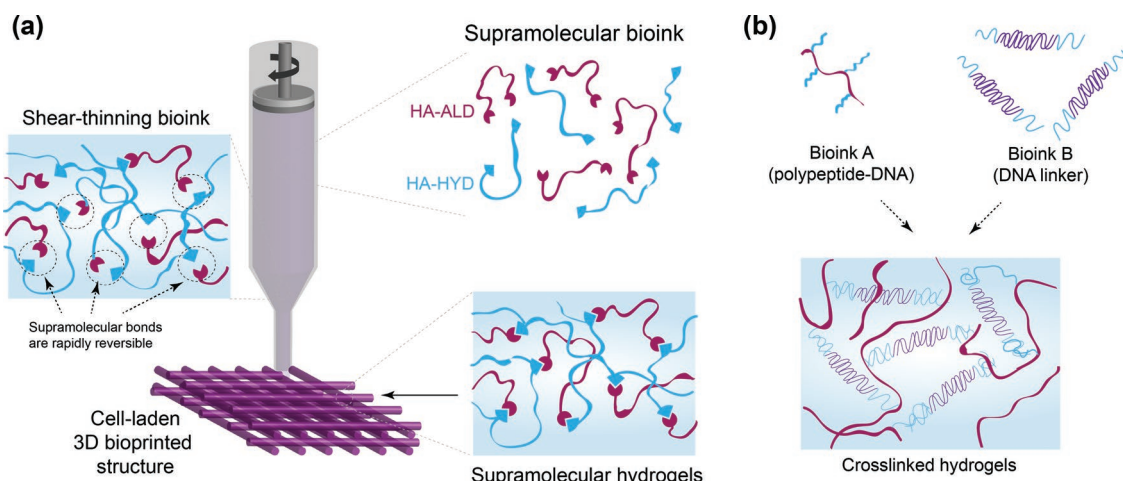
Figure 3. Supramolecular mechanisms for bioink reinforcement. a) Supramolecular bonds act as reversible crosslinks. They are disrupted when a crack propagates through the hydrogel, but quickly reform, regaining their strength. b) Complementary bioinks of polypeptide and DNA can be deposited alternatingly to obtain supramolecular 3D printed structure. These self-healing structures can encapsulate cells.

mechanically disrupted, they can re-form rapidly without permanent losses in performance.[72] These characteristics impact viscoelastic properties in interesting ways. For example, supramolecular networks demonstrate elastic properties below their yield point, but behave like a viscous liquid after yielding. After shear stress is removed, supramolecular hydrogels reform into an elastic solid. Developing models to correlate these flow properties with supramolecular structure is still an active area of research.[18,73,74] These properties have been used to develop a supramolecular bioink by modifying HA with adamantane (Ad) and β-cyclodextrin (β-CD) (Ad–HA and CD–HA). 3D printed structures that use these HA-based supramolecular bioinks are able to support formation of complex shapes.[72] However, it was difficult to obtain multilayered structures using HA-based supramolecular bioinks due to their limited mechanical properties.

Supramolecular bonds attract interest among bioink researchers because they combine the reversibility of physical bonds with the versatility and customization of covalent crosslinking techniques.[75] Supramolecular bonds differ from covalent bonds because they do not have permanent crosslinks. Instead, bonds between molecules exist in a dynamic equilibrium between the bound and unbound states, meaning that bonds are constantly breaking apart and re-forming. Two important factors help determine how this affects hydrogel behavior: bond lifetime and the equilibrium constant (K_{eq}). The equilibrium constant reflects the free energy difference between the bound and unbound states. Higher equilibrium constants favor extensive complexation within the network, which generally creates more connected, stronger hydrogels. Bond lifetime is a kinetic factor determined by the size of activation energy barriers and contributes to supramolecular hydrogels' time-dependent mechanical properties. Supramolecular bonds do not contribute to fracture energy when their lifetime is much smaller than the timescale of deformation, but they behave much like permanent bonds during more rapid deformation. These thermodynamic and kinetic factors help explain some of the unusual behaviors of supramolecular bioinks.[73] Supramolecular bioinks are sensitive to their environment, which can be

exploited for creating bioinks. For example, a supramolecular bioink was developed to undergo reversible thermal gelation over room temperature using a living cationic ring-opening polymerization mechanism.[76] This network notably demonstrated good mechanical properties for a thermally gelling bioink, having a storage modulus of 4 kPa.[76]

3.2.1. Bioink Based on Guest–Host Interactions

Despite their interesting properties, the application of many supramolecular hydrogels for bioprinting has been limited due to their weakened strength in the presence of water, which competitively binds with supramolecular functional groups.[73,77] In the past few years, stronger water-compatible bonds have been developed, and more mechanically stable supramolecular hydrogels are being investigated for bioprinting. Supramolecular moieties can be vulnerable to creep and erosion over time, so they are often combined with covalent crosslinks and other mechanical reinforcement strategies in bioinks. For example, supramolecular bioinks were recently combined with methacrylation functionalization as a method to reinforce a weak supramolecular bioink.[78] In this study, hyaluronic acid polymers were methacrylated for covalent crosslinking and also functionalized with either guest (adamantane) or host (b-cyclodextrin) moieties to enable supramolecular crosslinking. This dually crosslinkable network resulted in a self-healing bioink that could be stabilized for at least 30 d after printing using covalent crosslinking. In contrast, guest–host (GH) only gels relaxed too quickly to be printed effectively.[78,79]

Recently, the same GH bioinks were reinforced further by creating a supramolecularly reinforced dual-network bioink by adding a covalently crosslinked second network.[80] Compared to the methacrylated GH network (MethGH), a tethered interpenetrating network (MethGH-DN) reinforcement significantly improved mechanical properties, including compressive modulus (3 vs 11 kPa) and tensile toughness (2 vs 13 kJ m^{-3}). Reinforcement was maintained through successive

**ADVANCED
SCIENCE NEWS**

www.advancedsciencenews.com

**ADVANCED
MATERIALS**

www.advmat.de

compression cycles, and qualitative tests showed rapid healing within ≈1 s. Interestingly, the MethGH-DN was also superior to an interpenetrating network with a nonmethacrylated GH first network, particularly at low strain rates and cyclic compressions, which demonstrates that tethering the first network to the second can be used to prevent Mullins-type softening in supramolecular bioinks.[80]

3.2.2. Supramolecular Bioinks

Beyond these hybrid bioinks, supramolecular hydrogel research continues to advance. This may lead to an increase in pure supramolecular bioinks as well. One recent folate-based supramolecular bioink combines hydrogen bonding and π–π bond stacking with zinc coordination bonds to create a scaffold with a storage modulus as high as 100 kPa. Scaffolds were biocompatible and self-supporting, although their long-term shape stability remains to be investigated.[81] Another interesting recent approach combines dynamic and covalent crosslinking into a single moiety. Gallol antioxidants, which cause fruit browning, form dynamic hydrogen bonds with protein backbones that initially provide rapid self-healing and shear recovery properties to the bioink.[82] Over the course of a day, the gallol functional groups are gradually oxidized to form permanent covalent bonds. This allows a single functional group to operate as both a dynamic and covalent crosslinker depending on scaffold age.

Another class of supramolecular bioink is fabricated using polypeptide–DNA hydrogels. This study showed that by alternatingly depositing two complementary bioinks, a stable bioprinted structure loaded with cells can be obtained.[83] Interestingly, these relatively large 3D printed structures are able to retain their shapes up to several millimeters in height without collapse. Due to the presence of DNA building blocks, these gels have self-healing properties. However, stability of these hydrogels for long-term cell culture needs to be examined for future applications.

The ability to heal is common in living tissues; hence, bioinks capable of healing damage are attractive choices for implantable materials. Like many biological materials, supramolecular hydrogels are often made with noncovalent bonds between small, self-assembling blocks, which makes them an attractive option for biomedical applications, including drug delivery and injectable materials. However, the complex and often toxic preparation of these materials, as well as the lower strength of supramolecular interactions, has limited their application as bioinks. Recent advancements in the design of supramolecular hydrogels, as well as their combination with other reinforcement techniques, are making them an increasingly attractive choice for 3D bioprinting.

3.3. Interpenetrating Networks Bioinks

IPNs increase fracture energy (Γ), toughness, and stiffness through a highly heterogeneous hydrogel architecture. IPNs are composed of two separate polymer networks that are held together with covalent or ionic crosslinks or both (**Figure 4**). Although multiple types of IPNs are available, they can be classified into two major types: (a) double network (DNs), where both networks are held together with covalent crosslinks, and (b) ionic–covalent entanglement (ICE) networks, where the sacrificial network is crosslinked with physical bonds. DN and ICE hydrogel networks are structurally similar and the initial energy dissipation of both is described with essentially the same equation ($\Gamma_D = 2(U_{dc})(N_{dc})(h)$), although the energy required to de-crosslink the physical network (U_{dc}), is generally less than in covalent networks (U_f).[15] Comparing DN and ICE networks, we see several key mechanical differences. Thanks to their purely covalent structure, DNs have high bond energy, can remain elastic under 40%–50% deformation, are nearly independent of strain rate, and are less sensitive to environmental effects like temperature, ions, and pH. On the downside, their bond breaking is not reversible, so once sacrificial bonds are ruptured, the hydrogel's mechanical properties are determined only by the intact extensible network. This makes DNs susceptible to fatigue over repeated stress cycles. In contrast, ICE networks are more sensitive to environmental effects, display hysteresis at lower strains, and are more strain rate dependent. However, physical crosslinks in ICE networks can reform over time, allowing the hydrogel to regain sacrificial bonds.[16,84]

3.3.1. Ionic–Covalent Entanglement Bioinks

In bioinks, the most promising IPNs are formed through ICE. This is because conventional DN networks form over too long a timescale for bioprinting applications.[7] ICE hydrogels are formed with an ionically crosslinked rigid polymer and a covalently crosslinked elastic polymer. Using two distinct crosslinking mechanisms greatly reduces the time required to form the IPN.[7] This combination also replaces the loss of permanent sacrificial bonds with the reversible dissociation of ionic network crosslinks. This can be modeled as a continuous pulling apart of aggregated ionically crosslinked polymers, which can cause velocity-dependent fracture behaviors.[85]

The potential for these ICE physical crosslinks to reform over time as a mechanism for creating bioinks with increased toughness has led to increased interest within the bioink development field. For example, an ICE interpenetrating network composed of 2.5 wt% alginate and 20 wt% PEG was printed into a crosshatch pattern structure capable of expanding to 300% of its initial length. These hydrogels were able to partially recover their fracture energy after deformation when stored in a humid chamber for 24 h, but bioprinting was not attempted.[86] In a more recent study, an ICE network was used for bioprinting in combination with nanosilicates.[13] A 1% κCA physical network was combined with a 10% GelMA covalent network, causing a nearly three times increase in modulus (κCA: 12 kPa, κCA-GelMA: 35 kPa). ICE networks significantly decreased the brittleness of the κCA network, increasing maximum stress at 70% compression from 16 to 141 kPa, and improved recovery from 25% to 84% during a five-cycle compression test. Nanosilicate reinforcement of the ICE network improved mechanical properties even further. ICE networks have good potential for creating highly deformable, cytocompatible bioinks with increased toughness.[13,86]

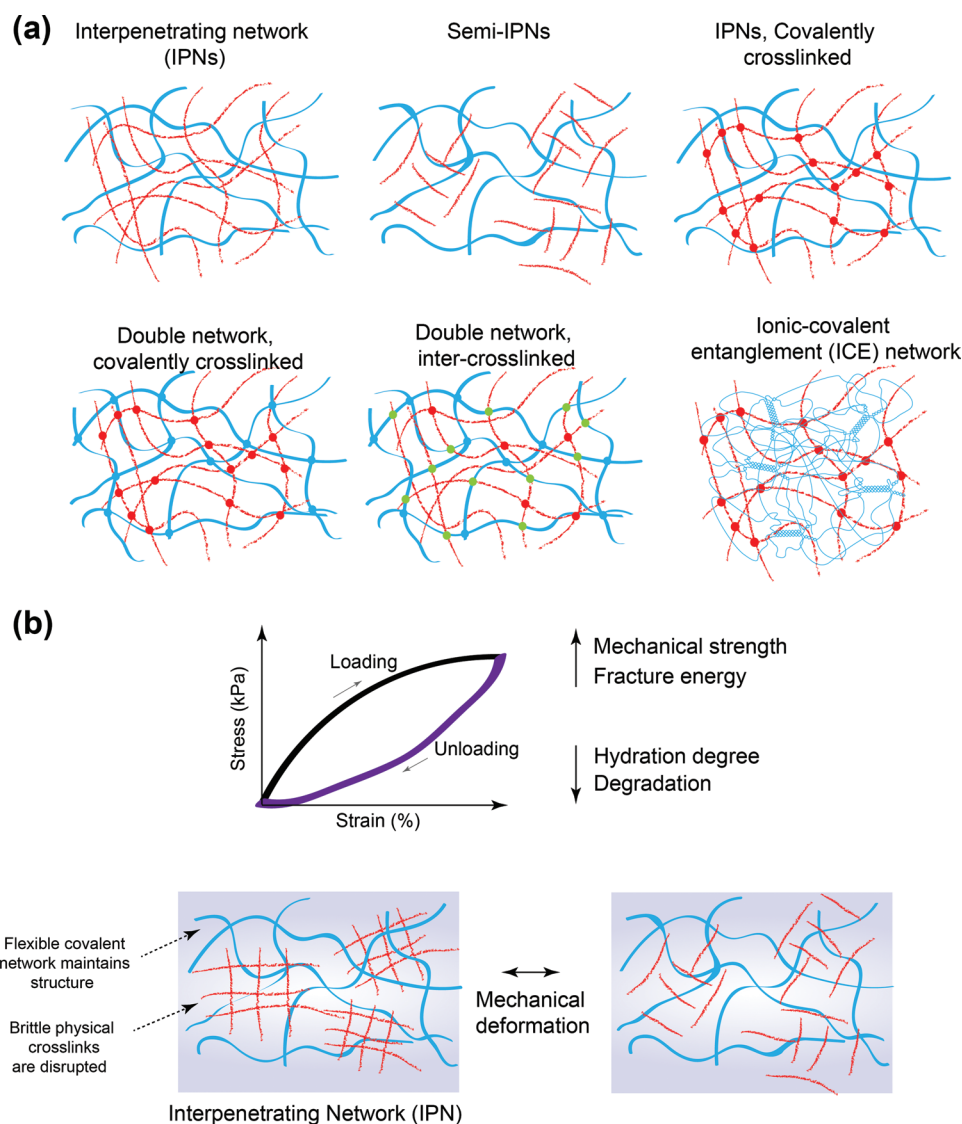Another example of an ICE network bioink was recently reported using 1.5% gellan gum and 10% PEGDA.[87] Gellan

**ADVANCED
SCIENCE NEWS**
www.advancedsciencenews.com

**ADVANCED
MATERIALS**
www.advmat.de

Figure 4. Bioink based on interpenetrating networks. a) Schematic demonstrating various types of interpenetrating networks. Interpenetrating networks are composed of two separate-but-entangled networks: one brittle network of sacrificial crosslinks, and one flexible, loosely crosslinked network. In Semi-IPNs, one network is not fully crosslinked. Some IPNs also contain some intercrosslinks that tether between networks. IPNs are called double networks (DNs) when both networks are covalently crosslinked, and ionic–covalent-entanglement networks (ICEs) when the sacrificial network is ionically crosslinked. ICE hydrogels represent most of the IPNs in bioprinting literature. b) The reversible sacrificial bonds present in ICEs provide high mechanical strength and fracture toughness compared to single network bioinks. In addition, many ICE networks are able to regain physical crosslinks over time, recovering stiffness.

gum is an anionic polysaccharide popular in bioprinting for its shear thinning properties and viscosity, but its application is limited by its brittleness and poor mechanical properties as a physically crosslinked single network. Gellan gum was incorporated into an ICE by adding a 10% PEGDA polymer network. Crosslinking the PEGDA network alone gave the bioink a 60 kPa compressive modulus and 34 kPa compressive strength, while allowing ions in the culture media to crosslink the gellan gum component increased these values to 184 and 55 kPa, respectively.[87] These studies demonstrate that ionically crosslinkable, high molecular weight polysaccharides like gellan gum and carrageenan are well suited for use

in ICE bioinks. Their molecular weight makes them effective viscosity modifiers useful for simultaneously improving both bioink flow and mechanical properties even at small polymer concentrations.[13,87]

3.3.2. Double Network Bioinks

In a recent study, a covalent-dynamic-covalent double network bioink was developed using two separate hyaluronic acid networks.[88] These dynamic-covalent interpenetrating networks are a promising method for combining the greater
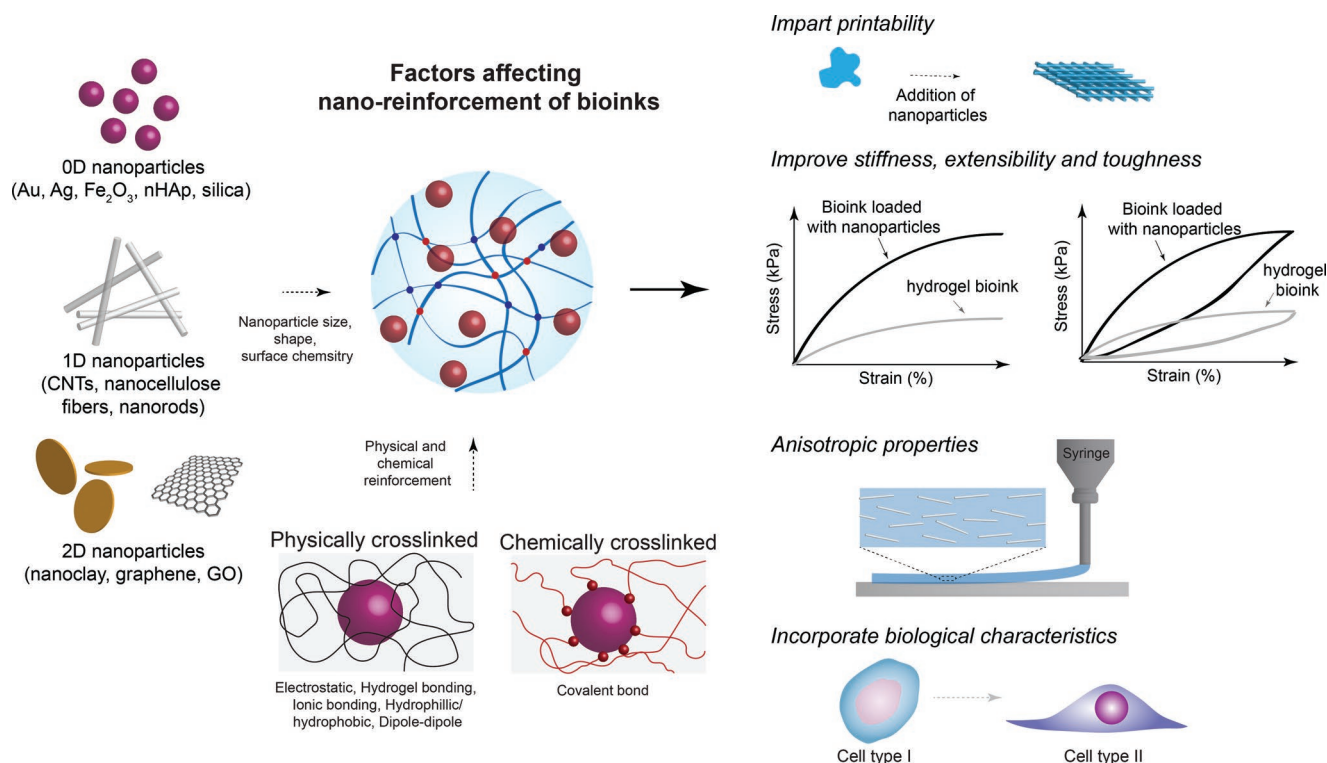
Figure 5. Bioink based on nanocomposite reinforcement. Nanoparticles with a range of sizes, shapes, and surface chemistries can mechanically reinforce bioinks through physical and covalent interactions. Nanoparticles reinforcement of hydrogel bioinks has been shown to improve printability, rheological properties, and mechanical properties. The use of anisotropic nanoparticles such as 1D or 2D nanomaterials in bioinks can imbue printed structures with anisotropic properties. Bioactive nanoparticles are able to direct cell function in 3D bioprinted structures. These bioactive effects occur through drug loading, direct interactions, or indirectly by affecting hydrogel viscoelastic properties.

bond strength of covalent bonds with the self-healing properties of ICEs. Hyaluronic acid was modified using two distinct methods to provide two independent networks via thiol-ene click crosslinking and hydrazone dynamic covalent bonds. This double network increased failure stress from 10 to 30 kPa over hydrazone crosslinking alone, and increased Young's modulus from 1 to 3 kPa. Additionally, bioprinted structures could be cut apart and recombined with other structures. After 10 min, the interfaces healed well enough that they could not be pulled apart manually. Near complete recovery of failure stress was attained after 30 min in 1.5 wt% hydrogels; however, recovery dropped to 50% upon increasing the composition to 3% hydrogel. This result suggests that denser hydrogels may require longer healing times or may not be completely recoverable. The authors hypothesize that restricted polymer mobility at higher concentrations may cause this effect. While the impact of double networking on the efficiency of the self-healing hydrazone bonds was not addressed, the use of dynamic covalent double networks represents an interesting new avenue of IPN research.[88]

In summary, IPNs improve mechanical properties by distributing mechanical energy over a broad damage zone using a brittle sacrificial network combined with an extensible second network. ICEs are being adopted for bioprinting because of their fast, cell-friendly formation and recoverable mechanical properties. The physically crosslinked polymer is also frequently a viscosity modifier, improving printability properties simultaneously.

3.4. Nanocomposite Reinforcement

Nanomaterials have rapidly gained interest within the biomedical engineering community over the past few years.[4,89,90] Due to their high specific surface area, even small concentrations of nanoparticles can significantly impact the properties of a hydrogel network.[89,91] The unique properties of nanomaterials have been exploited for many biomedical applications, including imaging, drug delivery, cancer therapies, and biosensor development. Incorporation of nanomaterials has been used to add new functionalities to bioinks, like enhanced electrical conductivity, stimuli responsiveness, control over cell behavior, printability improvements, and mechanical reinforcement.[7,89,91] A range of nanoparticles such as graphene, carbon nanotubes (CNTs), nanoclay, magnetic nanoparticles, transition metal dichalcogenides, and polymeric nanoparticles are extensively used to reinforce polymeric hydrogels and provide functionality.[4,90,92,93] The mechanism behind hydrogel nanomaterial reinforcement has also been a very active field of study.[94] The reinforcement mechanisms can vary depending on nanoparticle size, shape, and surface chemistry (**Figure 5**). Reinforcement of hydrogels is generally thought to occur through nanoparticles acting as reversible crosslinkers spanning multiple polymer chains. This allows stress to be efficiently dispersed across the network and dissipated through disruption of nanoparticle–polymer crosslinks. This mechanism has been shown to improve stiffness, extensibility, and

toughness of the nanoparticle-crosslinked hydrogels due to shorter polymer chains unbinding from the nanoparticle to dissipate stress, thus avoiding large-scale crack propagation.[14,15,94,95]

3.4.1. Nanoclay as Shear-Thinning Additive and Reinforcing Agent

Nanoclays (also known as nanosilicates) are the most widely used nanoparticles for bioink reinforcement,[12,94] and have been incorporated into a range of popular bioinks including alginate, PEG, GelMA, hyaluronic acid, and kappa carrageenan.[4,7,36] Their good water solubility and biocompatibility combined with their strong effects on rheological and mechanical properties have driven their popularity in bioink reinforcement.[89] Nanosilicates are disc-like 2D nanoplatelets less than 1 nm thick and can be synthesized from 25 nm to over 100 nm in diameter. Their crystal structure creates a permanent negative charge on both faces and permanent positive charges around the disc's edge. Nanosilicates' permanent surface charges and high specific surface area (>900 m^2 g^{-1}) enable them to form stable multifunctional networks of electrostatic crosslinks, which exist both between nanoclay particles and as nanoclay interactions with polymer strands.[94,96] These nanoclays are highly biocompatible and degrade in vitro and in vivo over time, making them appropriate for bioprinting application.[97]

During deformation, both nanoclay–nanoclay and nanoclay–polymer interactions can be reversibly disrupted to dissipate mechanical energy. Nanoclays can bind multiple polymer strands, allowing stress to be transferred between neighboring chains.[94] This load sharing greatly expands the damage zone around cracks and increases viscoelastic energy dissipation in nanosilicate reinforced hydrogels. Nanosilicates also cause substantial strain hardening by aligning during deformation, which blunts crack tips and makes hydrogels notch insensitive. Overall, small amounts of nanoclays can be used to significantly increase the fracture energy, stiffness, and extensibility of hydrogel networks.[89,94,96] In a recent publication, the compressive modulus of 2.5% kappa carrageenan was increased from 85 to 208 kPa with the inclusion of 6% nanoclay, without apparent harm to encapsulated cells over 7 d.[36]

The electrostatic interactions between nanoclay and polymer render bioinks with a reversible network structure that collapses during flow though the extruder and then rapidly re-forms after printing. This feature imbues bioinks with shear thinning and yield stress properties that are highly useful for bioprinting. Yield stress and shear thinning contribute to plug flow phenomena, where bioink is only fluid in a thin layer near the extruder walls while the bulk of the bioink extrudes as a solid. Because nanosilicates can bind multiple polymer chains together, their effects on flow properties are magnified in solutions containing polymers. This allows printability to be significantly improved by incorporating small amounts of nanosilicates and viscous polymer into the bioink. For example, while 10% GelMA is too fluid to print multilayer scaffolds, adding 2% nanosilicate and 1% κ-carrageenan as flow modifiers enables bioprinting of 3 cm tall, 150 layer structures.[13] Similar results have also been reported for an alginate–methylcellulose–nanosilicate bioink.[37]

Due to the ease of incorporating nanosilicates into aqueous solutions, nanosilicate reinforcement can be combined with other types of mechanical reinforcement techniques like supramolecular and ICE reinforced bioinks.[7,12,65,98] As an example, one co-printing study used 7% nanoclay to reinforce a 20% PEGDA structural ink co-printed with an osteoblast-laden 20% hyaluronic acid bioink for bone regeneration.[99] The inclusion of nanoclay increased compression modulus of printed scaffolds from 332 to 976 kPa. Each of these studies observed that the use of nanocomposite reinforcement improved both the mechanical properties and printability of the bioinks.[13,36,37,99] Interestingly, these nanoclay can also be used for prolonged and sustained delivery of therapeutics molecules, which is of significant advantage for bioprinting applications.[100]

3.4.2. Bioinks Reinforced with Nanofibers

Electrically conductive nanoparticles have also been investigated as bioink reinforcement. For example, carboxyl-functionalized multiwalled CNTs were covalently bonded to alginate to improve mechanical properties and electrical conductance of a methacrylated collagen scaffold for myocardial tissue engineering.[101] CNT nanocomposite scaffolds maintained physiological stability (43–54 kPa elastic modulus) over a 20 d culture period, while significantly reducing impedance at 5 Hz.[101] These CNT-reinforced bioprinted scaffolds improved cell proliferation and differentiation, suggesting that electrically conductive nanoreinforcement may be particularly suitable for myocardial tissue regeneration.[101] Graphene and its derivatives, graphene oxide (GO) and reduced graphene oxide (rGO), are noted for their use in reinforcing hydrogels and enhancing electrical conductivity, and are being widely adapted for biomedical applications including tissue engineering, drug delivery, and biosensing.[89] GO in particular is popular for its ease of functionalization and water solubility, and has been used to increase the compressive modulus of gelatin, chitosan, and alginate scaffolds. GO was recently used to reinforce a GelMA-PEGDA hydrogel (105 vs 135 kPa compressive modulus at 1 mg mL^{-1}) and induce chondrogenic differentiation of seeded human mesenchymal stem cells (hMSCs). rGO has also been used to reinforce GelMA from 2 to 23 kPa at 3 mg mL^{-1} in a scaffold for cardiac tissue engineering, while also improving cardiac beating and contractility among seeded cardiomyocytes.[89,102] GO has also been shown to improve printability of alginate by reducing layer sagging in printed structures.[103]

Other nanomaterials like cellulose nanofibers are also being investigated for bioink reinforcement. Cellulose nanofibers have high specific surface area and can form sacrificial hydrogen bonds that can be disrupted to dissipate stress.[7,104,105] Cellulose nanofiber reinforcement has been shown to increase the compressive modulus of a 5% GelMA bioink from <1 to 8 kPa by adding 2% cellulose nanofibers.[106] Their inclusion also improved bioink printability by increasing shear-thinning and zero shear viscosity. Similar success has also been reported using cellulose nanofibers to improve printability and mechanical properties in an alginate bioink.[107] More recently, promising results have also been reported using methylcellulose to nanoreinforce alginate and hyaluronic acid bioinks and

**ADVANCED
SCIENCE NEWS**

www.advancedsciencenews.com

**ADVANCED
MATERIALS**

www.advmat.de

improve printability.[108] Interestingly, a recent paper on nanocellulose fiber-polyethylene glycol dimethacrylate nanocomposites reports that cyclic preloading can cause nanocellulose fibers to rearrange and relax residual stresses, increasing fracture strength and crack initiation energy by over 20%, while decreasing modulus and fracture energy.[109]

3.4.3. Hydroxyapatite-Reinforced Bioinks

Hydroxyapatite nanoparticles are an attractive additive for tissue engineering because of their bone-like mineral content and osteogenic potential, which has led to increased popularity in nanocomposite bioinks.[5] In a recent study, incorporating 20 mg mL^{-1} nanohydroxyapatite increased elastic modulus in both 3% w/v alginate (3.5–18.8 kPa) and 2% w/v chitosan (4.6–15.0 kPa) nanocomposite bioinks.[110] Interestingly, the addition of hydroxyapatite nanoparticles to bioink formulation resulted in an increase low shear viscosity and shear thinning behavior. Hydroxyapatite nanoparticles also recover sufficient viscosity after extrusion to maintain printed shape fidelity, which was quantified using shear recovery tests. Overall, hydroxyapatite nanoparticles are popular in bone tissue engineering due to their bioactivity, but they also demonstrate significant mechanical and printability effects.[30,93,111]

3.4.4. Silica Nanoparticles as Reinforcing Agent

There has also been developing interest in synthesizing custom nanoparticles in order to better control the properties of bioinks. Silica nanoparticles were recently modified with aminopropyl groups to create cationic silica nanoparticles (AmNPs), creating strong electrostatic interactions between anionic polymers and the AmNPs.[112] This enhanced the zero-shear viscosity, shear-thinning properties, and yield stress of an alginate-gellan gum (3% and 3.5% w/v) bioink while maintaining rapid shear recovery. The 6% AmNP nanoreinforcement increased compressive modulus (≈50–85 kPa) and storage modulus (252–2390 kPa) over unreinforced bioink. This is a promising development because unmodified silica nanoparticles have very limited effect on mechanical properties, but cationic functionalization significantly improved interactions with the anionic bioink, demonstrating that the nanoreinforcement mechanism was due to electrostatic interactions. Interestingly, nanoreinforcement was improved by decreasing nanoparticle size and polymer chain length. This is likely because shorter polymer chains aggregate less and thus form more polymer–nanoparticle interactions, while smaller nanoparticle diameters have higher specific surface area so polymer chains are more likely to form interparticle, rather than intraparticle, bonds.[112,113]

3.4.5. Biocompatibility of Nanoengineered Bioinks

While improved printability and mechanical strength make nanocomposites popular for bioinks, the complexities of nanoparticle interactions pose difficult questions about how to evaluate their long-term biocompatibility. One major difficulty

is that at the nanoscale, material properties can change fundamentally with particle size, morphology, and functionalization, as well as chemical composition.[89,114] Differences in these properties can drastically affect nanomaterial interactions with biological systems at the subcellular level by altering cell uptake, degradability, and immunogenicity. This means that biocompatibility cannot be inferred from studies on bulk materials nor studies on nanoparticles of the same composition but different morphology. Consequently, there are contradictory studies on the biocompatibility of many nanomaterials, and a systematic understanding of their biological effects remains elusive. When evaluating nanomaterials for biocompatibility, it is important to match their morphology, functionalization, and composition, and to evaluate whether nanoparticles are behaving as expected during toxicity tests. Because nanoparticles can aggregate, form sediments, or remain disaggregated depending on environmental conditions, it is important to evaluate toxicity under conditions that match expected use. Finally, the novelty of nanomedicine has resulted in significant regulatory uncertainty as regulators have not yet established clear rules on evaluating nanomaterial safety, although this gap has been acknowledged and is being addressed by regulators. Overall, significant progress has been made in understanding in vitro and in vivo responses to various nanoparticles, but our understanding of nanomaterial biological interactions remains incomplete. Further research addressing this is necessary for translating this research into clinical applications.

3.5. Co-Printing and Thermoplastic Reinforcement

3.5.1. Thermoplastic Co-Printing

Thermoplastic 3D printed structures have been adopted for tissue engineering, typically as a macroporous structural support for cells. However, their inability to directly print cells has led to co-printing thermoplastics along with hydrogels. For example, thermoplastic can be printed first as the structural component to provide a mechanically stable scaffold, followed by printing cell-containing bioink.[115] Polycaprolactone (PCL) is the most common thermoplastic for co-printing because of its biocompatibility and relatively low melting temperature (60 °C), which allows co-extrusion with less risk of thermal injury to cells. In one recent work, a strong thermoplastic scaffold of PCL and tricalcium phosphate (compression modulus ≈40 kPa) was used for bone and cartilage regeneration, although it contained relatively small amounts of bioink.[115,116]

3.5.2. Hydrogel Co-Printing

One key limitation of thermoplastic co-printing is the inability to extrude fine thermoplastic filaments that interface effectively with hydrogels.[105] An interesting nonthermoplastic approach used for co-printing includes the use of a high-strength methacrylated poloxamer hydrogel alongside a 5% GelMA bioink (2.7 kPa).[25] This composite structure reached an overall stiffness of ≈200 kPa using 50 vol% of reinforcing gel.[25] This
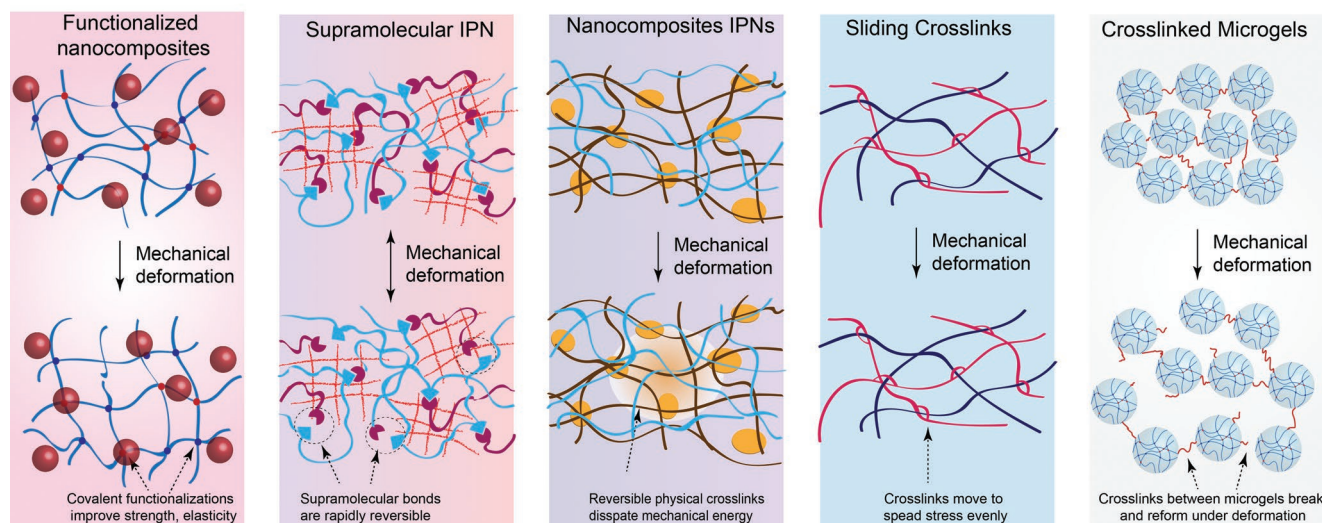
Figure 6. Emerging approaches for mechanical reinforcement. Combining reinforcement mechanisms together can provide bioinks with superior properties. Functionalized nanocomposites enable covalent nanoparticle interactions, which can improve strength and elasticity. Supramolecular IPNs can combine rapid supramolecular healing with the stability and strength of IPN networks. Nanoreinforcement of IPN networks results in very efficient bioink reinforcement with mechanical properties superior to either technique alone. Sliding crosslinks improve hydrogel extensibility by preventing stress concentrations, and could eventually be incorporated into bioinks. Crosslinked microgels are densely packed, or jammed, slurry of micrometer-scale hydrogel microspheres whose surfaces are crosslinked together after printing.

approach mitigates some of the disadvantages of thermoplastic reinforcement, including reduced diffusion and bioink-reinforcement interface issues, and potentially enables co-printing to be used for soft tissue implants as well.[25]

In a more recent study, a hydrogel support material was nano-reinforced to make a stiff scaffold for bone tissue regeneration. The bioink and support hydrogels were 20% hyaluronic acid solution and 20 wt% PEGDA + 7 wt% nanoclay (Laponite) (Laponite is a trademark of the company BYK Additives Ltd.) with a water content of only 74%, resulting in a water-stable and printable ink. Adding nanoclay increased the compressive modulus from 22 to 90 kPa, and increased compressive strength at 90% compression from 332 to 976 kPa. Hydrogel reinforcements like these provide advantages of thermoplastic co-printing while allowing better control over nutrient diffusion and degradation.[99]

3.5.3. Thermoplastic Microreinforcement

Micrometer-scale thermoplastics have also recently been explored as a bioink reinforcement. In this study, microfluidic fabrication was used to create sub-micrometer diameter PLA fibers that were suspended in an alginate bioink. This system was used to increase the Young's modulus of an alginate bioink by three to fourfold.[30] Microfiber reinforced bioinks also altered flow properties by increasing zero-shear viscosity. Interestingly, alginate present in the bioink dominates viscosity at higher shear rates.[30] Micrometer-scale thermoplastic fibers are finely integrated throughout the bioink, directly combining the load-bearing properties of thermoplastic reinforcement directly into the bioink, as opposed to an external support. This approach allows thermoplastic reinforcement to be applied to

soft tissues as well as bone, and improves bioink flow properties as well, although more research is needed to evaluate the generalizability of this promising technique.

The use of co-printed reinforcement remains an option for allowing the use of otherwise unprintable bioinks by extruding them onto a plastic support structure. While this technique can be applied to any bioink and can resemble the mechanical properties of hard tissues, challenges remain, particularly reduced nutrient diffusion, stress shielding, and separate degradation kinetics that may influence tissue regrowth. Alternatives are being developed to circumvent these problems. The development of smaller scale, more efficient reinforcement techniques can make co-printing more attractive for bioinks.

4. Emerging Trends and Future Directions

4.1. Combinatorial Bioinks (Multicomponent Bioinks)

One of the most promising future trends in mechanical bioink reinforcement is the combination of individual reinforcement techniques to make composite bioinks with interesting new properties. While individual reinforcement techniques laid out in this paper use very different strategies to improve the underlying mechanical properties of bioinks, many of the mechanisms behind these reinforcement strategies are not mutually exclusive and can be combined with other techniques, effectively creating new strategies that can compensate for weaknesses and integrate the strengths of different reinforcement mechanisms (**Figure 6**). Most combinatorial approaches are still in the beginning stages of development, but some interesting developments are already being published.

For example, supramolecularly functionalized HA was mixed with a covalently crosslinked methacrylated HA (Me-HA) to form an interpenetrating network.[80] While supramolecular networks are typically vulnerable to permanent deformation, the supramolecular polymers in this case were lightly tethered to the Me-HA network with covalent bonds. The cell-containing Me-HA single network's compressive modulus (2 kPa) was increased to 6 kPa as a supramolecular IPN network, and further increased to 11 kPa when the supramolecular network was covalently tethered to the covalent network. This design notably combines the mechanical properties of IPN reinforcement alongside the rapid self-healing of supramolecular polymers.[80]

Advancements in hydrogel reinforcement are also leading to interest in incorporating weaker materials efficiently into hydrogels. For example, a weak silk sericin hydrogel was recently incorporated into an interpenetrating network with GelMA for wound dressing applications.[117] In addition, incorporation of thermoresponsive components as polymer network or micro/nanoparticles can also incorporate stimuli-responsive characteristics along with mechanical reinforcement within bioink design.[118]

Nanocomposite reinforcement in particular is being combined with a number of other bioink reinforcement technologies because some materials like nanosilicates can be easily incorporated into aqueous solutions and affect both mechanical and flow properties of the bioink.[13] In this work, ionic–covalent-entanglement (10% GelMA and 1% kappa carrageenan) bioink was combined with nanosilicates (2%) to obtain a mechanically reinforced and highly printable nanoengineered-ICE bioink.[13] Interestingly, this study showed that reinforcement of GelMA (16.5 kPa) with either ICE or nSi reinforcement alone led to a roughly twofold increase in compressive modulus (≈35 kPa), while combining both together synergistically increased compressive modulus by fourfold to 71 kPa.[13]

Nanocomposite reinforcement has also been combined with supramolecular polymers to obtain elastomeric bioinks. For example, a poly(N-acryloyl glycinamide) (PNAGA)–nanoclay supramolecular hydrogel was developed for 3D printing scaffolds for bone tissue regeneration. The bioink was composed of 20 wt% PNAGA + 7 wt% nanoclay (Laponite), with a water content of only 74%, resulting in a water-stable, printable ink. The printed structure was mechanically stiff (compressive modulus 228 ± 10 kPa) and ductile, able to elongate to 1042 ± 97% of its relaxed length before breaking. The inclusion of nanoclay rendered the precursor printable and reinforced the hydrogels (228 vs 160 kPa without clay at 20% PNAGA). By relying on nanoclays for printability, the issue of poor printability of supramolecular precursors was overcome.[98]

4.2. Bioinks Based on Sliding Ring Crosslinks

One of the weaknesses of single network hydrogels is their heterogeneous network architecture. The random nature of their crosslinks causes stress concentration on the shortest chains, causing failure at lower strains than expected. In response, many efforts have been made to increase hydrogel homogeneity, notably through the use of mechanically interlocked molecules including sliding ring crosslink systems like polyrotaxanes.

These rings dynamically slide across chains to redistribute forces evenly among crosslinks to avoid stress concentrations throughout the network, resulting in hydrogels with superior extensibility and rupture strength (Figure 6). Most of these systems require noncytocompatible steps like high temperatures or dimethyl sulfoxide (DMSO) use because polyrotaxane is insoluble in water, and so this approach has not yet gained much traction for biomedical applications. However, recently a new sliding crosslinker has been developed that incorporates succinic functional groups onto the polyrotaxane, rendering it water soluble.[119] This allowed a cytocompatible 3D culture of hMSCs in the sliding hydrogel with a compressive modulus of 10 kPa. This technology could be adapted for bioprinting as it continues to develop more simple and cytocompatible methods, especially as more research is done on the effect of sliding crosslink hydrogels on encapsulated cell behavior.[14,119,120]

4.3. Bioink Based on Hydrogel Microspheres

Another upcoming trend worth discussing is the emergence of hydrogel microsphere bioinks. These bioinks are a densely packed, or jammed, slurry of micrometer-scale hydrogel microspheres whose surfaces can be crosslinked together after extrusion. This approach allows porosity to be controlled independently of bioink composition, enabling highly interconnected, microporous scaffolds to be created while also providing a stiff microenvironment for cells.[121–123] Microsphere printing can also be used to build heterogeneous scaffolds using microspheres with different compositions and encapsulated cells.[122,124,125] Recent publications have reported using microspheres with different stiffnesses to affect fibroblast proliferation and spreading,[122] and creating mixtures of microspheres containing either osteo or chondrogenically differentiated mesenchymal stem cells.[124] Microspheres used in this way may enable micrometer-scale heterogeneity to be incorporated into bioprinted scaffolds without requiring micrometer-scale resolution.[125]

Some recent publications have demonstrated encouraging printability results using microsphere bioinks, including centimeter-scale freestanding scaffolds.[124–126] Shear thinning, yield stress, and shear recovery properties have also been reported; however, the factors behind microsphere printability remain poorly understood. Variables including microsphere size, polydispersity, packing density, surface interactions, and suspension medium may affect printability, but more research is necessary to evaluate these factors.[127,128] The increased porosity of microsphere scaffolds also reduces their mechanical properties, with one study reporting a reduction in compressive modulus from 15 to 5 kPa when comparing conventional hydrogel scaffolds to crosslinked microspheres.[128] However, there has been very little investigation into the mechanical properties of microsphere scaffolds. The dependence of a scaffold's bulk mechanical properties on factors like particle packing, void fraction, microparticle mechanical properties, size distribution, particle–particle contact area, and crosslinking will require systematic investigation to better understand their application to bioprinting. Bioprinting hydrogel microspheres represents an interesting new approach to incorporate micrometer-scale porosity and heterogeneity into bioinks, and early in vivo tests on injected microspheres report

improved vascularization and wound healing in skin lesions compared to conventional hydrogel.[123,129] These encouraging results are likely to facilitate more research into microsphere bioprinting.

4.4. Micrometer-Scale Thermoplastic Reinforcement

In contrast to the macroscale thermoplastic reinforcement discussed earlier, which acts as structures containing hydrogel, smaller nano and microscale fibers can be incorporated into hydrogel bioinks to alter the hydrogel's mechanical properties. For example, melt electrospinning writing (MEW) can form highly porous and fibrous scaffolds of nanofibers to mimic native tissue microstructure using melted polymer instead of conventional volatile solvent solutions.[130–132] In one recent study, MEW was used to deposit a micrometer-scale thermoplastic network that increased Young's modulus by 18-fold over the PEG + heparin hydrogel network alone, while taking up only 5.6% of the scaffold volume. This reinforcement was caused by the thermoplastic network restricting hydrogel swelling, thereby enabling compressive forces to be transferred to the thermoplastic network as tensile stress. This design is reminiscent of cartilage's architecture, and the dynamic mechanical properties of the scaffolds showed similar responses to loading over time to cartilage, suggesting that mimicking the structural architecture of cartilage tissue may help us replicate its physical properties.[131,133]

However, it should be noted that these scaffolds were molded and not bioprinted. Despite its attractive properties, MEW is not compatible with bioprinting in its current form because printing speed is too slow, where even a small volume can take many hours,[25] and the presence of hydrogel on the build plate could interfere with the MEW process. MEW has not been combined with bioprinting for these reasons, but its incorporation into the bioprinting toolkit could be very beneficial for obtaining high strength bioprints in the future.[131,133]

Nevertheless, biocompatible incorporation of small-scale fibers into bioinks can significantly affect mechanical properties, as demonstrated by the recent reinforcement of an alginate bioink with sub-micrometer PLA fibers.[30] Similar techniques may be more easily adopted to co-bioprinting than electrospinning, like Solution Blow Spinning (SBS), which does not require an electric field and deposits much more quickly. SBS has been used to deposit poly(lactic-co-glycolic acid) nanofibers in situ during surgery and is gaining popularity in tissue engineering for its ease of use and biocompatibility; however, the literature surrounding SBS is still light.[134] It remains to be seen whether MEW, SBS, or other technologies will successfully incorporate micrometer-scale thermoplastics into bioprinting, but the potential advantages of finer interfacing between bioprinting and thermoplastics remain a compelling avenue for new reinforcement techniques.[130,135]
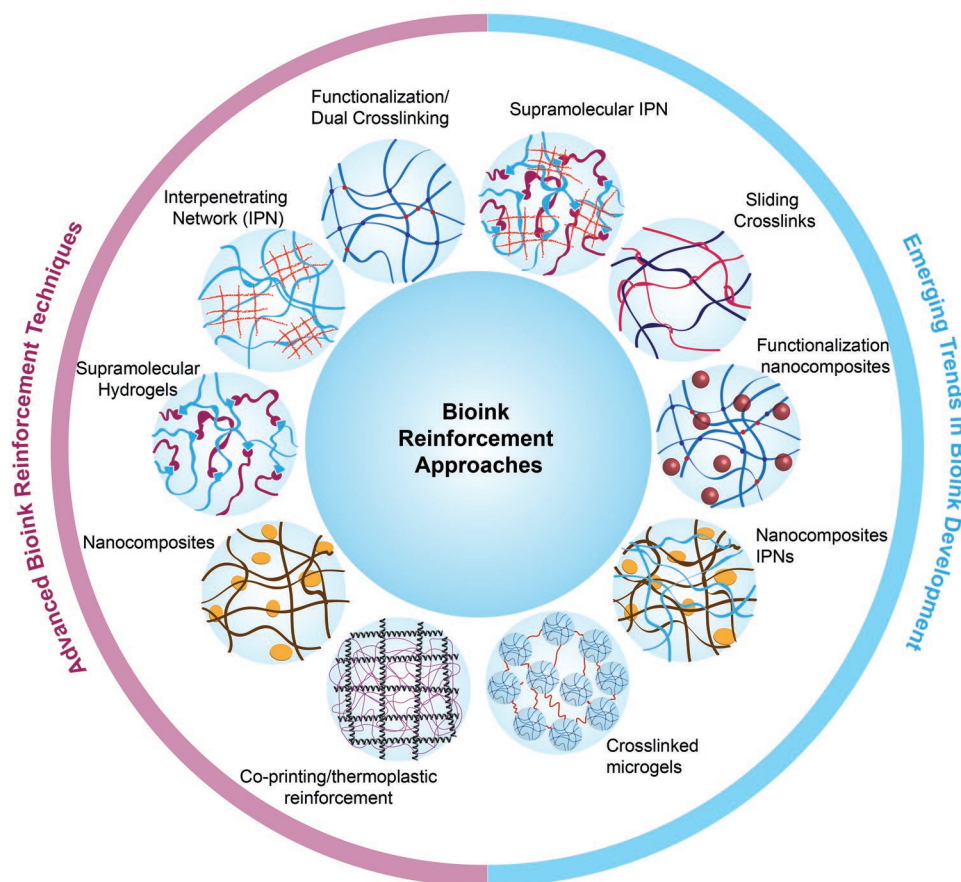

Figure 7. Current and emerging approaches in bioink reinforcement.

5. Conclusion

Bioinks are specialized hydrogels used to dispense suspended cells into 3D support scaffolds. The specific environmental needs of living cells pull bioinks toward dilute networks, while mechanical and flow requirements improve with higher polymer concentrations. These contradicting requirements are driving research into more advanced hydrogel designs and have raised exciting questions about efficient bioink reinforcement. Conventional single network hydrogels have neither the intrinsic fracture energy (Γ_0) nor the mechanical energy dissipation (Γ_D) capabilities of other polymer networks and are further weakened by stress concentrations arising from their random network structure. Techniques that incorporate mechanical energy dissipation mechanisms into the hydrogel structure can dramatically improve fracture energy with only modest changes in composition. Nearly all bioink reinforcement to date uses this strategy in some form (**Figure 7**). For example, polymer functionalization increases intrinsic fracture energy (Γ_0) by strengthening crosslinks, while interpenetrating networks, nanocomposites, and supramolecular approaches increase mechanical energy dissipation (Γ_D) capabilities by enabling applied stress to be mechanically dissipated without damaging the main network. Many of these techniques also allow ruptured bonds to heal over time, whether through reconstitution of physical bonds in ionic–covalent entanglement networks, reversible electrostatic interactions among nanoparticles and polymer chains, or by reestablishing the dynamic equilibrium of supramolecular bonds. Each of these reinforcement techniques has their own impacts on bioink viscoelastic properties, which was discussed in detail. However, exact properties are controlled by specific network architecture (polymer concentrations, identities, crosslink mechanisms, chain lengths, isotropy) and environmental properties (temperature, ion concentrations, pH), as well as strain rate, direction, and processing history. Looking forward, interest in bioink reinforcement approaches is expanding as its interactions with cell behavior and flow properties become clear. Combinations of multiple reinforcement techniques are expanding, and early reports indicate that combined reinforcement may have synergistic effects. New approaches like microsphere bioprinting and sliding ring crosslinks are on the horizon as well. As bioink performance improves, the promise of creating custom 3D reconstructions of patient tissue will continue to push bioprinting from the bench to the clinical bedside. From a regulatory perspective, bioprinted scaffolds will be complex to regulate, since they can be simultaneously biologics, drugs, and medical devices. Fortunately, regulatory agencies have been generally proactive at providing guidelines, since it is recognized that overcoming these obstacles will be necessary for bringing 3D bioprinting toward the eventual goal of clinical use to improve patient lives.

Conflict of Interest

The authors declare no conflict of interest.

Keywords

[1] C. W. Hull, *US 4575330A*, **1986**.

[2] S. S. Crump, *US 5121329A*, **1992**.

[3] a) L. Moroni, J. A. Burdick, C. Highley, S. J. Lee, Y. Morimoto, S. Takeuchi, J. J. Yoo, *Nat. Rev. Mater.* **2018**, *3*, 21; b) C. J. Ferris, K. G. Gilmore, G. G. Wallace, *Appl. Microbiol. Biotechnol.* **2013**, *97*, 4243; c) P. Zorlutuna, N. Annabi, G. Camci-Unal, M. Nikkhah, J. M. Cha, J. W. Nichol, A. Manbachi, H. Bae, S. Chen, A. Khademhosseini, *Adv. Mater.* **2012**, *24*, 1782.

[4] A. K. Gaharwar, L. M. Cross, C. W. Peak, K. Gold, J. K. Carrow, A. Brokesh, K. A. Singh, *Adv. Mater.* **2019**, *31*, 1900332.

[5] N. Ashammakhi, A. Hasan, O. Kaarela, B. Byambaa, A. Sheikhi, A. K. Gaharwar, A. Khademhosseini, *Adv. Healthcare Mater.* **2019**, *8*, 1801048.

[6] a) R. R. Jose, M. J. Rodriguez, T. A. Dixon, F. Omenetto, D. L. Kaplan, *ACS Biomater. Sci. Eng.* **2016**, *2*, 1662; b) A. K. Gaharwar, A. Arpanaei, T. L. Andresen, A. Dolatshahi-Pirouz, *Adv. Mater.* **2016**, *28*, 771.

[7] D. Chimene, K. K. Lennox, R. R. Kaunas, A. K. Gaharwar, *Ann. Biomed. Eng.* **2016**, *44*, 2090.

[8] J. Malda, J. Visser, F. P. Melchels, T. Jüngst, W. E. Hennink, W. J. A. Dhert, J. Groll, D. W. Hutmacher, *Adv. Mater.* **2013**, *25*, 5011.

[9] O. Z. Fisher, A. Khademhosseini, R. Langer, N. A. Peppas, *Acc. Chem. Res.* **2010**, *43*, 419.

[10] B. V. Slaughter, S. S. Khurshid, O. Z. Fisher, A. Khademhosseini, N. A. Peppas, *Adv. Mater.* **2009**, *21*, 3307.

[11] N. Annabi, A. Tamayol, J. A. Uquillas, M. Akbari, L. E. Bertassoni, C. Cha, G. Camci-Unal, M. R. Dokmeci, N. A. Peppas, A. Khademhosseini, *Adv. Mater.* **2014**, *26*, 85.

[12] A. Vedadghavami, F. Minooei, M. H. Mohammadi, S. Khetani, A. R. Kolahchi, S. Mashayekhan, A. Sanati-Nezhad, *Acta Biomater.* **2017**, *62*, 42.

[13] D. Chimene, C. W. Peak, J. Gentry, J. K. Carrow, L. M. Cross, E. Mondragon, G. B. C. Cardoso, R. Kaunas, A. K. Gaharwar, *ACS Appl. Mater. Interfaces* **2018**, *10*, 9957.

[14] C. Creton, *Macromolecules* **2017**, *50*, 8297.

[15] X. Zhao, *Soft Matter* **2014**, *10*, 672.

[16] R. Long, C.-Y. Hui, *Soft Matter* **2016**, *12*, 8069.

[17] B. N. J. Persson, O. Albohr, G. Heinrich, H. Ueba, *J. Phys.: Condens. Matter* **2005**, *17*, R1071.

[18] C. Creton, M. Ciccotti, *Rep. Prog. Phys.* **2016**, *79*, 046601.

[19] O. Wichterle, D. Lím, *Nature* **1960**, *185*, 117.

[20] S. C. Lee, I. K. Kwon, K. Park, *Adv. Drug Delivery Rev.* **2013**, *65*, 17.

[21] D. A. Foyt, M. D. Norman, T. T. Yu, E. Gentleman, *Adv. Healthcare Mater.* **2018**, *7*, 1700939.

[22] D. Maugis, M. Barquins, *J. Phys. D: Appl. Phys.* **1978**, *11*, 1989.

[23] T. Zhang, S. Lin, H. Yuk, X. Zhao, *Extreme Mech. Lett.* **2015**, *4*, 1.

[24] V. H. Mouser, F. P. Melchels, J. Visser, W. J. Dhert, D. Gawlitta, J. Malda, *Biofabrication* **2016**, *8*, 035003.

[25] F. P. Melchels, M. M. Blokzijl, R. Levato, Q. C. Peiffer, M. De Ruijter, W. E. Hennink, T. Vermonden, J. Malda, *Biofabrication* **2016**, *8*, 035004.

[26] N. Paxton, W. Smolan, T. Böck, F. Melchels, J. Groll, T. Jungst, *Biofabrication* **2017**, *9*, 044107.

[27] L. Ning, A. Guillemot, J. Zhao, G. Kipouros, X. Chen, *Tissue Eng., Part C* **2016**, *22*, 652.

[28] M. Sarker, X. B. Chen, *J. Manuf. Sci. Eng.* **2017**, *139*, 081002.

[29] F. P. Melchels, W. J. Dhert, D. W. Hutmacher, J. Malda, *J. Mater. Chem. B* **2014**, *2*, 2282.

[30] A. Kosik-Kozioł, M. Costantini, T. Bolek, K. Szöke, A. Barbetta, J. Brinchmann, W. Święszkowski, *Biofabrication* **2017**, *9*, 044105.

[31] S. Sathaye, A. Mbi, C. Sonmez, Y. Chen, D. L. Blair, J. P. Schneider, D. J. Pochan, *Wiley Interdiscip. Rev.: Nanomed. Nanobiotechnol.* **2015**, *7*, 34.

[32] M. A. Rao, in *Rheology of Fluid, Semisolid, and Solid Foods* (Ed: M. A. Rao), Springer, New York **2014**, p. 27.

[33] H. A. Barnes, *J. Non-Newtonian Fluid Mech.* **1997**, *70*, 1.

[34] S. Kyle, Z. M. Jessop, A. Al-Sabah, I. S. Whitaker, *Adv. Healthcare Mater.* **2017**, *6*, 1700264.

[35] Y. Jin, C. Liu, W. Chai, A. Compaan, Y. Huang, *ACS Appl. Mater. Interfaces* **2017**, *9*, 17456.

[36] S. A. Wilson, L. M. Cross, C. W. Peak, A. K. Gaharwar, *ACS Appl. Mater. Interfaces* **2017**, *9*, 43449.

[37] T. Ahlfeld, G. Cidonio, D. Kilian, S. Duin, A. Akkineni, J. Dawson, S. Yang, A. Lode, R. Oreffo, M. Gelinsky, *Biofabrication* **2017**, *9*, 034103.

[38] C. W. Peak, J. Stein, K. A. Gold, A. K. Gaharwar, *Langmuir* **2017**, *34*, 917.

[39] V. H. Mouser, A. Abbadessa, R. Levato, W. Hennink, T. Vermonden, D. Gawlitta, J. Malda, *Biofabrication* **2017**, *9*, 015026.

[40] J. S. Park, J. S. Chu, A. D. Tsou, R. Diop, Z. Tang, A. Wang, S. Li, *Biomaterials* **2011**, *32*, 3921.

[41] G. Huang, F. Li, X. Zhao, Y. Ma, Y. Li, M. Lin, G. Jin, T. J. Lu, G. M. Genin, F. Xu, *Chem. Rev.* **2017**, *117*, 12764.

[42] A. J. Engler, S. Sen, H. L. Sweeney, D. E. Discher, *Cell* **2006**, *126*, 677.

[43] N. Huebsch, P. R. Arany, A. S. Mao, D. Shvartsman, O. A. Ali, S. A. Bencherif, J. Rivera-Feliciano, D. J. Mooney, *Nat. Mater.* **2010**, *9*, 518.

[44] A. Bauer, L. Gu, B. Kwee, W. A. Li, M. Dellacherie, A. D. Celiz, D. J. Mooney, *Acta Biomater.* **2017**, *62*, 82.

[45] O. Chaudhuri, L. Gu, D. Klumpers, M. Darnell, S. A. Bencherif, J. C. Weaver, N. Huebsch, H.-P. Lee, E. Lippens, G. N. Duda, D. J. Mooney, *Nat. Mater.* **2016**, *15*, 326.

[46] R. Goetzke, A. Sechi, L. De Laporte, S. Neuss, W. Wagner, *Cell. Mol. Life Sci.* **2018**, *75*, 3297.

[47] K. H. Vining, D. J. Mooney, *Nat. Rev. Mol. Cell Biol.* **2017**, *18*, 728.

[48] F. Guilak, D. M. Cohen, B. T. Estes, J. M. Gimble, W. Liedtke, C. S. Chen, *Cell Stem Cell* **2009**, *5*, 17.

[49] J. K. Mouw, J. T. Connelly, C. G. Wilson, K. E. Michael, M. E. Levenston, *Stem Cells* **2007**, *25*, 655.

[50] A. Tondon, R. Kaunas, *PLoS One* **2014**, *9*, e89592.

[51] Y. Li, K. A. Kilian, *Adv. Healthcare Mater.* **2015**, *4*, 2780.

[52] K. J. France, F. Xu, T. Hoare, *Adv. Healthcare Mater.* **2018**, *7*, 1700927.

[53] A. J. Steward, D. J. Kelly, *J. Anat.* **2015**, *227*, 717.

[54] C. W. Peak, S. Nagar, R. D. Watts, G. Schmidt, *Macromolecules* **2014**, *47*, 6408.

[55] J. Lou, R. Stowers, S. Nam, Y. Xia, O. Chaudhuri, *Biomaterials* **2018**, *154*, 213.

[56] Y. S. Zhang, A. Khademhosseini, *Science* **2017**, *356*, eaaf3627.

[57] R. F. Pereira, P. J. Bártolo, *J. Appl. Polym. Sci.* **2015**, *132*, 42458.

[58] H. Shirahama, B. H. Lee, L. P. Tan, N.-J. Cho, *Sci. Rep.* **2016**, *6*, 31036.

[59] B. H. Lee, H. Shirahama, N.-J. Cho, L. P. Tan, *RSC Adv.* **2015**, *5*, 106094.

[60] W. Liu, M. A. Heinrich, Y. Zhou, A. Akpek, N. Hu, X. Liu, X. Guan, Z. Zhong, X. Jin, A. Khademhosseini, Y. S. Zhang, *Adv. Healthcare Mater.* **2017**, *6*, 1601451.

[61] B. J. Klotz, D. Gawlitta, A. J. Rosenberg, J. Malda, F. P. Melchels, *Trends Biotechnol.* **2016**, *34*, 394.

[62] L. E. Bertassoni, J. C. Cardoso, V. Manoharan, A. L. Cristino, N. S. Bhise, W. A. Araujo, P. Zorlutuna, N. E. Vrana, A. M. Ghaemmaghami, M. R. Dokmeci, *Biofabrication* **2014**, *6*, 024105.

[63] L. Ouyang, C. B. Highley, W. Sun, J. A. Burdick, *Adv. Mater.* **2017**, *29*, 1604983.

[64] a) K. Yue, G. Trujillo-de Santiago, M. M. Alvarez, A. Tamayol, N. Annabi, A. Khademhosseini, *Biomaterials* **2015**, *73*, 254; b) S. M. Mihaila, A. K. Gaharwar, R. L. Reis, A. P. Marques, M. E. Gomes, A. Khademhosseini, *Adv. Healthcare Mater.* **2013**, *2*, 895.

[65] A. Thakur, M. K. Jaiswal, C. W. Peak, J. K. Carrow, J. Gentry, A. Dolatshahi-Pirouz, A. K. Gaharwar, *Nanoscale* **2016**, *8*, 12362.

[66] M. Rizwan, G. S. Peh, H.-P. Ang, N. C. Lwin, K. Adnan, J. S. Mehta, W. S. Tan, E. K. Yim, *Biomaterials* **2017**, *120*, 139.

[67] S. Bertlein, G. Brown, K. S. Lim, T. Jungst, T. Boeck, T. Blunk, J. Tessmar, G. J. Hooper, T. B. Woodfield, J. Groll, *Adv. Mater.* **2017**, *29*, 1703404.

[68] S. Stichler, S. Bertlein, J. Tessmar, T. Jüngst, J. Groll, *Macromolecular Symp.* **2017**, *372*, 102.

[69] T. E. Brown, K. S. Anseth, *Chem. Soc. Rev.* **2017**, *46*, 6532.

[70] a) S. Stichler, T. Jungst, M. Schamel, I. Zilkowski, M. Kuhlmann, T. Böck, T. Blunk, J. Teßmar, J. Groll, *Ann. Biomed. Eng.* **2017**, *45*, 273; b) M. W. Tibbitt, A. M. Kloxin, L. A. Sawicki, K. S. Anseth, *Macromolecules* **2013**, *46*, 2785; c) K. Vats, G. Marsh, K. Harding, I. Zampetakis, R. E. Waugh, D. S. Benoit, *J. Biomed. Mater. Res., Part A* **2017**, *105*, 1112.

[71] a) S. Das, F. Pati, Y.-J. Choi, G. Rijal, J.-H. Shim, S. W. Kim, A. R. Ray, D.-W. Cho, S. Ghosh, *Acta Biomater.* **2015**, *11*, 233; b) Y. Shi, T. L. Xing, H. B. Zhang, R. X. Yin, S. M. Yang, J. Wei, W. J. Zhang, *Biomed. Mater.* **2018**, *13*, 035008.

[72] C. B. Highley, C. B. Rodell, J. A. Burdick, *Adv. Mater.* **2015**, *27*, 5075.

[73] J. L. Mann, C. Y. Anthony, G. Agmon, E. A. Appel, *Biomater. Sci.* **2018**, *6*, 10.

[74] E. A. Appel, J. del Barrio, X. J. Loh, O. A. Scherman, *Chem. Soc. Rev.* **2012**, *41*, 6195.

[75] S. Seiffert, J. Sprakel, *Chem. Soc. Rev.* **2012**, *41*, 909.

[76] T. Lorson, S. Jaksch, M. M. Lübtow, T. Jüngst, J. Groll, T. Lühmann, R. Luxenhofer, *Biomacromolecules* **2017**, *18*, 2161.

[77] X. Dai, Y. Zhang, L. Gao, T. Bai, W. Wang, Y. Cui, W. Liu, *Adv. Mater.* **2015**, *27*, 3566.

[78] C. Loebel, C. B. Rodell, M. H. Chen, J. A. Burdick, *Nat. Protoc.* **2017**, *12*, 1521.

[79] L. Ouyang, C. B. Highley, C. B. Rodell, W. Sun, J. A. Burdick, *ACS Biomater. Sci. Eng.* **2016**, *2*, 1743.

[80] C. B. Rodell, N. N. Dusaj, C. B. Highley, J. A. Burdick, *Adv. Mater.* **2016**, *28*, 8419.

[81] K. Liu, S. Zang, R. Xue, J. Yang, L. Wang, J. Huang, Y. Yan, *ACS Appl. Mater. Interfaces* **2018**, *10*, 4530.

[82] M. Shin, J. H. Galarraga, M. Y. Kwon, H. Lee, J. A. Burdick, *Acta Biomater.* **2018**, *95*, 165.

[83] C. Li, A. Faulkner-Jones, A. R. Dun, J. Jin, P. Chen, Y. Xing, Z. Yang, Z. Li, W. Shu, D. Liu, *Angew. Chem.* **2015**, *127*, 4029.

[84] J. P. Gong, *Science* **2014**, *344*, 161.

[85] Q. Chen, H. Chen, L. Zhu, J. Zheng, *Macromol. Chem. Phys.* **2016**, *217*, 1022.

[86] S. Hong, D. Sycks, H. F. Chan, S. Lin, G. P. Lopez, F. Guilak, K. W. Leong, X. Zhao, *Adv. Mater.* **2015**, *27*, 4035.

[87] D. Wu, Y. Yu, J. Tan, L. Huang, B. Luo, L. Lu, C. Zhou, *Mater. Des.* **2018**, *160*, 486.

[88] L. L. Wang, C. B. Highley, Y. C. Yeh, J. H. Galarraga, S. Uman, J. A. Burdick, *J. Biomed. Mater. Res., Part A* **2018**, *106*, 865.

[89] D. Chimene, D. L. Alge, A. K. Gaharwar, *Adv. Mater.* **2015**, *27*, 7261.

[90] A. K. Gaharwar, N. A. Peppas, A. Khademhosseini, *Biotechnol. Bioeng.* **2014**, *111*, 441.

[91] F. Bonaccorso, L. Colombo, G. Yu, M. Stoller, V. Tozzini, A. C. Ferrari, R. S. Ruoff, V. Pellegrini, *Science* **2015**, *347*, 1246501.

[92] a) M. K. Jaiswal, J. K. Carrow, J. L. Gentry, J. Gupta, N. Altangerel, M. Scully, A. K. Gaharwar, *Adv. Mater.* **2017**, *29*, 1702037; b) M. Parani, G. Lokhande, A. Singh, A. K. Gaharwar, *ACS Appl. Mater. Interfaces* **2016**, *8*, 10049.

[93] T. Thakur, J. R. Xavier, L. Cross, M. K. Jaiswal, E. Mondragon, R. Kaunas, A. K. Gaharwar, *J. Biomed. Mater. Res., Part A* **2016**, *104*, 879.

[94] A. Klein, P. G. Whitten, K. Resch, G. Pinter, *J. Polym. Sci., Part B: Polym. Phys.* **2015**, *53*, 1763.

[95] H. Xin, H. R. Brown, S. Naficy, G. M. Spinks, *J. Polym. Sci., Part B: Polym. Phys.* **2016**, *54*, 53.

[96] T. Nishida, A. Obayashi, K. Haraguchi, M. Shibayama, *Polymer* **2012**, *53*, 4533.

[97] a) J. K. Carrow, L. M. Cross, R. W. Reese, M. K. Jaiswal, C. A. Gregory, R. Kaunas, I. Singh, A. K. Gaharwar, *Proc. Natl. Acad. Sci. USA* **2018**, *115*, E3905; b) A. K. Gaharwar, R. K. Avery, A. Assmann, A. Paul, G. H. McKinley, A. Khademhosseini, B. D. Olsen, *ACS Nano* **2014**, *8*, 9833; c) A. K. Gaharwar, S. M. Mihaila, A. Swami, A. Patel, S. Sant, R. L. Reis, A. P. Marques, M. E. Gomes, A. Khademhosseini, *Adv. Mater.* **2013**, *25*, 3329.

[98] X. Zhai, Y. Ma, C. Hou, F. Gao, Y. Zhang, C. Ruan, H. Pan, W. W. Lu, W. Liu, *ACS Biomater. Sci. Eng.* **2017**, *3*, 1109.

[99] X. Zhai, C. Ruan, Y. Ma, D. Cheng, M. Wu, W. Liu, X. Zhao, H. Pan, W. W. Lu, *Adv. Sci.* **2017**, *5*, 1700550.

[100] a) C. W. Peak, K. A. Singh, M. A. Adlouni, J. Chen, A. K. Gaharwar, *Adv. Healthcare Mater.* **2019**, *8*, 1801553; b) L. M. Cross, J. K. Carrow, X. Ding, K. A. Singh, A. K. Gaharwar, *ACS Appl. Mater. Interfaces* **2019**, *11*, 6741; c) A. Sheikhi, S. Afewerki, R. Oklu, A. K. Gaharwar, A. Khademhosseini, *Biomater. Sci.* **2018**, *6*, 2073; d) G. Lokhande, J. K. Carrow, T. Thakur, J. R. Xavier, M. Parani, K. J. Bayless, A. K. Gaharwar, *Acta Biomater.* **2018**, *70*, 35; e) D. W. Howell, C. W. Peak, K. J. Bayless, A. K. Gaharwar, *Adv. Biosyst.* **2018**, *2*, 1870061.

[101] M. Izadifar, D. Chapman, P. Babyn, X. Chen, M. E. Kelly, *Tissue Eng., Part C* **2017**, *24*, 74.

[102] a) X. Zhou, M. Nowicki, H. Cui, W. Zhu, X. Fang, S. Miao, S.-J. Lee, M. Keidar, L. G. Zhang, *Carbon* **2017**, *116*, 615; b) S. R. Shin, C. Zihlmann, M. Akbari, P. Assawes, L. Cheung, K. Zhang, V. Manoharan, Y. S. Zhang, M. Yüksekkaya, K. T. Wan, *Small* **2016**, *12*, 3677; c) C.-T. Huang, L. K. Shrestha, K. Ariga, S.-h. Hsu, *J. Mater. Chem. B* **2017**, *5*, 8854.

[103] H. Li, S. Liu, L. Lin, *Int. J. Bioprinting* **2016**, *2*, 13.

[104] J. Yang, C.-R. Han, J.-F. Duan, F. Xu, R.-C. Sun, *ACS Appl. Mater. Interfaces* **2013**, *5*, 3199.

[105] G. Chinga-Carrasco, *Biomacromolecules* **2018**, *19*, 701.

[106] S. Shin, S. Park, M. Park, E. Jeong, K. Na, H. J. Youn, J. Hyun, *BioResources* **2017**, *12*, 2941.

[107] K. Markstedt, A. Mantas, I. Tournier, H. Martínez Ávila, D. Hägg, P. Gatenholm, *Biomacromolecules* **2015**, *16*, 1489.

[108] a) A. Habib, V. Sathish, S. Mallik, B. Khoda, *Materials* **2018**, *11*, 454; b) N. Law, B. Doney, H. Glover, Y. Qin, Z. M. Aman, T. B. Sercombe, L. J. Liew, R. J. Dilley, B. J. Doyle, *J. Mech. Behav. Biomed. Mater.* **2018**, *77*, 389.

[109] C. S. Wyss, P. Karami, P.-E. Bourban, D. P. Pioletti, *Extreme Mech. Lett.* **2018**, *24*, 66.

[110] D. Tuğrul Tolga, I. Gülseren, G. Menemşe, *Biofabrication* **2017**, *9*, 035003.

[111] a) S. T. Bendtsen, S. P. Quinnell, M. Wei, *J. Biomed. Mater. Res., Part A* **2017**, *105*, 1457; b) Z. Meng, T. Thakur, C. Chitrakar, M. K. Jaiswal, A. K. Gaharwar, V. V. Yakovlev, *ACS Nano* **2017**, *11*, 7690.

[112] M. Lee, K. Bae, P. Guillon, J. Chang, Ø. Arlov, M. Zenobi-Wong, *ACS Appl. Mater. Interfaces* **2018**, *10*, 37820.

[113] E. A. Appel, M. W. Tibbitt, M. J. Webber, B. A. Mattix, O. Veiseh, R. Langer, *Nat. Commun.* **2015**, *6*, 6295.

[114] J. Wolfram, M. Zhu, Y. Yang, J. Shen, E. Gentile, D. Paolino, M. Fresta, G. Nie, C. Chen, H. Shen, *Curr. Drug Targets* **2015**, *16*, 1671.

[115] H.-W. Kang, S. J. Lee, I. K. Ko, C. Kengla, J. J. Yoo, A. Atala, *Nat. Biotechnol.* **2016**, *34*, 312.

[116] K. Zhang, Q. Fu, J. Yoo, X. Chen, P. Chandra, X. Mo, L. Song, A. Atala, W. Zhao, *Acta Biomater.* **2017**, *50*, 154.

[117] C.-S. Chen, F. Zeng, X. Xiao, Z. Wang, X.-L. Li, R.-W. Tan, W.-Q. Liu, Y.-S. Zhang, Z.-D. She, S.-J. Li, *ACS Appl. Mater. Interfaces* **2018**, *10*, 33879.

[118] a) N. A. Jalili, M. K. Jaiswal, C. W. Peak, L. M. Cross, A. K. Gaharwar, *Nanoscale* **2017**, *9*, 15379; b) N. A. Jalili, M. Muscarello, A. K. Gaharwar, *Bioeng. Transl. Med.* **2016**, *1*, 297.

[119] X. Tong, F. Yang, *Adv. Mater.* **2016**, *28*, 7257.

[120] a) I. Bin, *Chem. Commun.* **2016**, *52*, 13757; b) L. Jiang, C. Liu, K. Mayumi, K. Kato, H. Yokoyama, K. Ito, *Chem. Mater.* **2018**, *30*, 5013.

[121] A. Sheikhi, J. de Rutte, R. Haghniaz, O. Akouissi, A. Sohrabi, D. Di Carlo, A. Khademhosseini, *Biomaterials* **2019**, *192*, 560.

[122] J. M. de Rutte, J. Koh, D. Di Carlo, *Adv. Funct. Mater.* **2019**, *29*, 1970174.

[123] L. Riley, L. Schirmer, T. Segura, *Curr. Opin. Biotechnol.* **2019**, *60*, 1.

[124] O. Jeon, Y. B. Lee, T. J. Hinton, A. W. Feinberg, E. Alsberg, *Mater. Today Chem.* **2019**, *12*, 61.

[125] a) C. B. Highley, K. H. Song, A. C. Daly, J. A. Burdick, *Adv. Sci.* **2019**, *6*, 1801076; b) J. E. Mealy, J. J. Chung, H. H. Jeong, D. Issadore, D. Lee, P. Atluri, J. A. Burdick, *Adv. Mater.* **2018**, *30*, 1705912.

[126] S. Xin, D. Chimene, J. E. Garza, A. K. Gaharwar, D. L. Alge, *Biomater. Sci.* **2019**, *7*, 1179.

[127] J. E. Mealy, J. J. Chung, H.-H. Jeong, D. Issadore, D. Lee, P. Atluri, J. A. Burdick, *Adv. Mater.* **2018**, *30*, 1705912.

[128] C. B. Highley, K. H. Song, A. C. Daly, J. A. Burdick, *Adv. Sci.* **2018**, *6*, 1801076.

[129] D. R. Griffin, W. M. Weaver, P. O. Scumpia, D. Di Carlo, T. Segura, *Nat. Mater.* **2015**, *14*, 737.

[130] J. L. Daristotle, A. M. Behrens, A. D. Sandler, P. Kofinas, *ACS Appl. Mater. Interfaces* **2016**, *8*, 34951.

[131] a) J. Visser, F. P. Melchels, J. E. Jeon, E. M. Van Bussel, L. S. Kimpton, H. M. Byrne, W. J. Dhert, P. D. Dalton, D. W. Hutmacher, J. Malda, *Nat. Commun.* **2015**, *6*, 6933; b) O. Bas, E. M. De-Juan-Pardo, C. Meinert, D. D'Angella, J. G. Baldwin, L. J. Bray, R. M. Wellard, S. Kollmannsberger, E. Rank, C. Werner, *Biofabrication* **2017**, *9*, 025014.

[132] a) O. Bas, E. M. De-Juan-Pardo, M. P. Chhaya, F. M. Wunner, J. E. Jeon, T. J. Klein, D. W. Hutmacher, *Eur. Polym. J.* **2015**, *72*,

451; b) O. Bas, S. Lucarotti, D. D. Angella, N. J. Castro, C. Meinert, F. M. Wunner, E. Rank, G. Vozzi, T. J. Klein, I. Catelas, *Chem. Eng. J.* **2018**, *340*, 15.

[133] P. D. Dalton, *Curr. Opin. Biomed. Eng.* **2017**, *2*, 49.

[134] A. M. Behrens, B. J. Casey, M. J. Sikorski, K. L. Wu, W. Tutak, A. D. Sandler, P. Kofinas, *ACS Macro Lett.* **2014**, *3*, 249.

[135] C. Chen, A. D. Townsend, S. A. Sell, R. S. Martin, *Anal. Methods* **2017**, *9*, 3274.